

5-2018

# Involvement of the INO80 Complex in Chromosome Segregation

Jesus Moreno

*University of Arkansas, Fayetteville*

Follow this and additional works at: <http://scholarworks.uark.edu/etd>

 Part of the [Genomics Commons](#), [Molecular Biology Commons](#), and the [Molecular Genetics Commons](#)

---

## Recommended Citation

Moreno, Jesus, "Involvement of the INO80 Complex in Chromosome Segregation" (2018). *Theses and Dissertations*. 2753.  
<http://scholarworks.uark.edu/etd/2753>

This Thesis is brought to you for free and open access by ScholarWorks@UARK. It has been accepted for inclusion in Theses and Dissertations by an authorized administrator of ScholarWorks@UARK. For more information, please contact [scholar@uark.edu](mailto:scholar@uark.edu), [ccmiddle@uark.edu](mailto:ccmiddle@uark.edu).

Involvement of the INO80 Complex in Chromosome Segregation

A thesis submitted in partial fulfillment  
of the requirements for the degree of  
Master of Science in Cell and Molecular Biology

by

Jesus Moreno  
Universidad Autonoma de Chiriqui  
Bachelor of Science in Chemistry, 2014

May 2018  
University of Arkansas

This thesis is approved for recommendation to the Graduate Council

---

Ines Pinto, Ph.D.  
Thesis Director

---

Mack Ivey, Ph.D.  
Committee Member

---

Josh Sakon, Ph.D.  
Committee Member

## ABSTRACT

Chromatin remodeling complexes are multi-protein complexes that regulate the dynamics of the nucleosomes in the genome. The INO80 chromatin remodeling complex participates in varied biological processes such as: transcription, DNA repair, DNA replication and chromosome integrity. It catalyzes the eviction of the H2A.Z variant histone as well as whole nucleosome eviction. This complex is comprised of 15 subunits and the contribution of each to chromosome segregations remains unknown. To evaluate the contribution of each subunit to chromosome segregation, we tested deletion mutants of the non-essential subunits for DNA content and benomyl sensitivity. Also, we assessed members of the SWR1 and NuA4 complexes which relate to the same substrate. Additionally, specific members of the complex were tested for genetic interaction with *SGO1*. The deletion of *INO80*, *ARP5*, *ARP8*, *IES6* and *TAF14* cause increased ploidy and increased benomyl sensitivity. Additionally, overexpression of *SGO1* suppresses the benomyl sensitivity and possibly protects the cell from diploidization. Overall, specific subunits of the complex play a role in chromosome segregation and defects caused by mutants of INO80 could be alleviated by *SGO1*-mediated bi-orientation.

## ACKNOWLEDGEMENTS

I would like to thank Dr. Ines Pinto for her mentorship throughout the Master Degree process. I am very grateful for her guidance in the lab techniques and her teaching oriented to work independently and think critically. I would like to thank Dr. David McNabb for his suggestions and input throughout the thesis project.

## DEDICATION

This dedication is dedicated to my parents, Walter Moreno and Rosmery de Moreno, and my brother, Walter Moreno for their personal sacrifice and support to achieve my academic and personal goals. I would like to mention my friends, Zane Sarma, Tanny Chavez, Sergio Mosquera, Sittie Aisha and David Cajias, for been a family away from home, their support and friendship.

## TABLE OF CONTENTS

I.	INTRODUCTION.....	1
II.	LITERATURE REVIEW.....	3
	a. <i>Saccharomyces cerevisiae</i> as a model organism.....	4
	b. Chromatin characteristics.....	5
	c. Histones, post-translational modifications and function.....	6
	d. Histone variants.....	9
	e. Chromatin remodeling complexes.....	12
	f. The INO80 complex.....	13
	g. Chromosome segregation.....	15
	h. Sgo1.....	16
III.	METHODS.....	18
	a. <i>Saccharomyces cerevisiae</i> strains and media .....	19
	b. <i>Escherichia coli</i> strains and media.....	19
	c. Design of 13-Myc plasmid with Nat <sup>R</sup> marker.....	20
	d. Double mutant construction.....	20
	e. Benomyl sensitivity assay.....	21
	f. Canavanine assay of ploidy.....	21
	g. Flow cytometry.....	21
	h. Chromatin Immunoprecipitation assay.....	22
IV.	RESULTS.....	23
	a. Specific subunits of complexes INO80 and SWR1 affect ploidy.....	24
	b. Ploidy increase correlates with benomyl sensitivity.....	25

c.	Interaction of the INO80 complex with <i>SGO1</i> .....	26
d.	Overexpression of <i>SGO1</i> suppresses benomyl sensitivity of specific subunits of INO80.....	29
e.	Loss of Arp8 doesn't affect pericentromeric binding of Ino80.....	30
V.	DISCUSSIONS.....	31
a.	Specific subunits of INO80 and SWR1 involved in chromosome segregation.....	32
b.	Analysis of subunit contribution to the INO80 complex in chromosome segregation.....	33
c.	Differential genetic interaction of <i>ARP5</i> and <i>ARP8</i> with <i>SGO1</i> relevant to chromosome segregation.....	35
d.	INO80 conserves pericentromeric binding upon <i>ARP8</i> deletion.....	36
VI.	REFERENCES.....	60

## **I. INTRODUCTION**



The cell undergoes several maintenance and regulatory processes to preserve its proper function. The conservation of the integrity of the genome belongs to one of these regulatory processes. It is of significant value for cells to preserve the integrity of their genetic information. Alterations can be transmitted through cell division, propagate the error further and lead to detrimental conditions to the cell's function. This premise underlies the importance of understanding the mechanism of segregation of chromosomes during mitosis. It is important to employ a simple model organism to begin the description of the principles that govern chromosome segregation in complex organisms. The budding yeast *Saccharomyces cerevisiae* represents a simple yet relevant model to study chromosome segregation. In this work, I will examine the involvement of the chromatin remodeling complex INO80 in chromosome segregation.

The INO80 complex, along with other chromatin remodeling complexes, dynamically controls chromatin structure by modification of the histone composition of the nucleosomes. Previous work on the Ies6 subunit of INO80 shows a possible remodeling function of the pericentromere and ploidy maintenance, which could link the complex to chromosome segregation (Chambers et al., 2012). The objective of this research is to describe the contribution of the subunits of the INO80 complex to chromosome segregation and to determine whether these subunits associate with the pericentromeric regions within chromosomes. The involvement of the complex in chromosome segregation was assessed by creating deletion mutants of the non-essential subunits of the complex. The location of the complex was determined by chromatin immunoprecipitation. The results indicate that specific subunits of the INO80 complex affect chromosome segregation and affect ploidy status of the cell. Also, some subunits show genetic interactions with *SGO1*. Overall, the contribution of these subunits reflects important biochemical and biological functions of the complex relevant for maintaining chromosome stability.

**II. LITERATURE REVIEW**

## ***Saccharomyces cerevisiae* as a model organism**

The budding yeast, *Saccharomyces cerevisiae*, is one of the most studied models for genetics and molecular biology. *S. cerevisiae*'s genome was the first eukaryotic genome completely sequenced. The complete sequence of *S. cerevisiae* has helped progress the discovery of homologous proteins and molecular pathways in metazoans, contributing to understanding conserved mechanisms in biology. Referred to as baker's or budding yeast, this unicellular eukaryote presents several advantages as a model based on the simplicity of the genome, life cycle and versatility as an organism.

The genome of *S. cerevisiae* is comprised of 5915 ORFs distributed within sixteen chromosomes of varied lengths (Goffeau et al., 1996). Compared to the genomes of higher metazoans, the budding yeast holds a compact genome of approximately 12 Mbp with about 70 % corresponding to ORFs. Additionally, the genome presents a low frequency of introns, about 4 % of the protein-encoding genes, which makes it a simple model organism to mutate and assess gene and protein function. Notably, the characterization of the genes in yeast has given great insight in the function of homologous genes, conserved molecular mechanisms in higher metazoan species, gene interactions, gene evolution and diseases (Botstein & Fink, 2011).

The life cycle of this budding yeast provides great advantage for molecular and genetic studies. *S. cerevisiae* can exist as both stable haploid and diploid which divide mitotically. Also, the duplication time last about two hours, making it a fast organism to grow and analyze. Under starvation, the diploid undergoes meiosis through the process of sporulation, producing four haploid spores contained in an ascus, making the process genetically tractable.

## Chromatin characteristics

The genome of the cell should be kept with high fidelity for the maintenance of proper biological functions. The information stored in the genome requires a dynamic regulation by adequate activation/deactivation of genes based on the need of the cell. In eukaryotes, this regulation is achieved by structural control of the genome and selectively altering the accessibility of genes. The structural units of the genome are chromosomes and the structural arrangement is called chromatin. Chromatin comprises the DNA and interacting proteins that allow control over the compaction of chromatin. Based on compaction, chromatin can be classified in heterochromatin and euchromatin. In the following sections, the characteristics of chromatin, its components and factors that affect it are discussed.

The compaction of chromatin plays an important role in the cell cycle and transcription of genes. Heterochromatin correlates with silencing of genes and euchromatin with actively transcribed genes. In metazoans, chromatin adopts several structural organizations depending on the level of compaction. The basal level is provided by the DNA associated with histone proteins to form the nucleosome, forming the 11 nm “beads on a string” structure, followed by 30 nm fibers and higher order structures (G. Li & Reinberg, 2011). Distinct models have been proposed for the 30 nm fibers and higher order structures, yet those structures remain poorly characterized (Bian & Belmont, 2012; G. Li & Reinberg, 2011). *S. cerevisiae* contain a simpler organization of chromatin and serve as model organism to study heterochromatin and its genomic distribution. Heterochromatin in yeast localizes in particular genomic regions, the telomeres and the mating type loci (HML, HMR), and highly regulated by silencer regions, post-translational modifications (PTM) of the nucleosome and protein interaction with the chromatin (Bi, 2014; Bühler & Gasser, 2009).

Besides heterochromatin and euchromatin, chromosomes exhibit a distinct region called centromere, involved in the chromosome segregation and genome integrity. The centromeres act as anchors for the microtubules to guide the transport of chromosomes during cell division. In metazoans, large regional satellite repeats define the centromeres and contain multiple attachments with the microtubules during mitosis (Verdaasdonk & Bloom, 2011). However, *S. cerevisiae*'s centromeres are characterized by specific DNA sequences and one attachment with microtubules. This DNA sequences are called as centromere DNA elements I, II and III (CDEI, CDEII, CDEII), extending about 120 bps (Clarke & Carbon, 1983). Additionally, the CDEs locates within close distance from the ORF of proteins, rDNAs and autonomous replication sequences.

### **Histones, post-translational modifications and functions**

The nucleosome is the basic structure that forms chromatin. The nucleosome comprised of DNA and an octamer formed by two copies of the H2A, H2B, H4 and H3 histones. The DNA segment of 146 bp wraps around the octameric histone with left handed superhelical turn forming the core particle of the nucleosome (Luger, Mäder, Richmond, Sargent, & Richmond, 1997). The histones share a common structure, comprised by N- and C- terminal extensions between a histone fold motif characterized by three  $\alpha$  helices connected through loops (McGinty & Tan, 2015). The N-terminals of the histones protrude for the core particle and mediate interactions with the chromatin and chromatin-interacting proteins. As the building block of chromatin, nucleosome dynamics control the organization of the genome mediated by PTMs, histone variants and chromatin remodeling.

The function of PTMs depends on the type of modification, location within the nucleosome and the genome. Histones undergo various PTMs such as acetylation, methylation,

phosphorylation, ubiquitination, sumoylation, ADP ribosylation among others (Prakash & Fournier, 2018; Strahl & Allis, 2000). Typically, PTMs are incorporated in the nucleosome by a “writer” enzyme and controlled by an “eraser” (Jaiswal, Turniansky, & Green, 2017). Careful balance between the eraser and the writer enzymes regulate the cell functions associated with the PTM. Additionally, some PTMs regulate the occurrence of other modifications; this is defined as the cross-talk between PTMs. Also, the location of histones and their PTM becomes especially relevant in the yeast genome due to the low distance between genes.

### Methylation and acetylation

Methylation and acetylation belong to one of the most characterized modifications, particularly because of its occurrence and role in transcription. These modifications can define active or inactive genes by their location, for example H3K4me<sub>3</sub>, H3K9Ac, H3K14Ac and N-terminal acetylation of H4 (K5, K6, K12 and K16) predominantly localize in the transcription start site of active genes (Pokholok et al., 2005). Likewise, H3K36me<sub>3</sub> and H3K79me<sub>3</sub> distribute within the body of genes. Alternatively, the silent heterochromatin of telomeres and HM loci represent another case of localized regulation of PTMs, characterized by hypoacetylation of H4K16 and hypomethylation in H3K4 and H3K79 (Bi, 2014; Thurtle & Rine, 2014). Therefore, both methylation and acetylation describe the dynamic state of chromatin during transcription. Besides transcription, these PTMs participate in other cellular processes (Williamson & Pinto, 2012). Acetylation occurs in cell cycle events, in the assembly of the nucleosome and chromosome condensation, in H3K56 and H3K16 respectively (Darieva, Webber, Warwood, & Sharrocks, 2015; Q. Li et al., 2008; Wilkins et al., 2014). Interestingly, both H3K56 and H3K16 are mediated by a previous histone phosphorylation, describing the cross talk between PTM in the regulation of diverse cell processes.

## Phosphorylation

Phosphorylation displays a wide variety of functions in the cell and some are conserved among eukaryotes (Rossetto, Avvakumov, & Cote, 2012). In mammals, the repertoire of histone phosphorylation exceeds the ones in yeast, however functions such as DNA repair, meiosis, apoptosis and chromosome condensation remains conserved and linked to histone phosphorylation (Banerjee & Chakravarti, 2011; Rossetto et al., 2012). Similar to methylation and acetylation, phosphorylation occurs in the four canonical histones. H3 displays phosphorylation in Thr45 during DNA replication (Darieva et al., 2015). Phosphorylation of H3S10 occurs during G2/M stage and meiosis and linked to chromosome condensation (Hsu et al., 2000). Similarly, H2BS10 phosphorylation increases during meiosis as well as apoptosis (Ahn, Henderson, Keeney, & Allis, 2005). Interestingly, promoter phosphorylation of H2B in Tyr40 represses the expression of histones (Mahajan, Fang, Koomen, & Mahajan, 2012). In the fission yeast, the H2AS121 phosphorylation regulates the location of Shugoshin (S. A. Kawashima, Yamagishi, Honda, Ishiguro, & Watanabe, 2010), a protein linked to sensing chromosome tension during chromosome segregation. Phosphorylation has been highly studied by its role in DNA damage shown by H4S1 and H2AS129 phosphorylation (Cheung et al., 2005; Downs et al., 2004; van Attikum, Fritsch, Hohn, & Gasser, 2004). Particularly, H2AS129 phosphorylation assist the recruitment of the NuA4, Swr1 and Ino80 complex to DNA damage sites (Downs et al., 2004; van Attikum et al., 2004).

## Ubiquitination

Unlike most small size PTMs, ubiquitin adds a 76-amino acid and about 8.5 kDa protein to the nucleosome. Ubiquitination of H2A occurs in Lys119 in eukaryotes, yet absent in yeast (J. Cao & Yan, 2012). H2B displays ubiquitilation in Lys 123 in yeast (Robzyk, Recht, & Osley,

2000), which correspond to Lys120 in humans. Ubiquitin is commonly associated with protein degradation; however, histone ubiquitination displays alternative cellular functions. For instance, H2A ubiquitination has been associated with gene repression (Nakagawa et al., 2008).

Ubiquitination of H2B acts as positive regulator of specific methylations, by H2Bub promoted methylation through Set1 and Dot1 of H3K4 and H3K79, respectively; (Ng, Xu, Zhang, & Struhl, 2002; Sun & Allis, 2002) and reduced chromatin binding of Jhd2, the H3K4 demethylase (Huang et al., 2015). Alternatively, it displays negative regulation by Set2 inhibition resulting in decrease of H4K36 methylation (Wyce et al., 2007). Also, H2B ubiquitination stabilizes nucleosomal positioning, coordinates transcription of genes based of its genomic position and regulates the spread of H3K36 throughout the genome (Batta, Zhang, Yen, Goffman, & Pugh, 2011).

## **Histone variants**

### **Cse4**

The *CSE4* gene was initially characterized as a gene involve in chromosome segregation with homology with the H3 histone and human CENP-A (Stoler, Keith, Curnick, & Fitzgerald-Hayes, 1995). Also, shares structural similarities within the histone fold domain required for the centromere nucleosome (Morey, Barnes, Chen, Fitzgerald-Hayes, & Baker, 2004) as well as N- and C-terminal extensions. Because incorporation of Cse4 into chromatin marks centromere formation, the localization of this variant requires a careful regulation. Cse4's deposition in the chromosomes occurs during S phase (Pearson et al., 2004), additionally a more recent study suggests a second deposition during late anaphase to form a centromere with two copies of Cse4 (Shivaraju et al., 2012). Cell cycle control of Cse4 is mediated by degradation



through ubiquitylation of both N-and C-terminal extensions (Au, Crisp, DeLuca, Rando, & Basrai, 2008; Au et al., 2013).

To maintain correct chromosome segregation, Cse4 require several regulatory mechanisms. A dosage-dependent control of H3 and Cse4 is required for accurate genomic localization and segregation (Au et al., 2008). Defects in Cse4 turnover and increased stability of Cse4 display chromosome segregation problems (Au et al., 2008; Au et al., 2013). Additionally, phosphorylation of Cse4 regulates chromosome segregation under microtubule attachment stress (Boeckmann et al., 2013). Overall, localization, dosage and phosphorylation of Cse4 participate to regulate correct chromosome segregation.

## H2A.Z

The H2A.Z variant shares 63% identity with the canonical H2A histone, however exhibits diverse characteristics and functions within the cell. Additionally, H2A.Z is expressed constitutively within the cell cycle, in contrast to the S phase expression of the canonical histone. This variant is highly conserved among metazoans and essential in some species (Billon & Côté, 2013). In budding yeast, the H2A.Z coding gene, HTZ1, is not essential allowing to describe its interaction with other genes and cell processes. H2A.Z contributes to a variety of cell processes such as DNA replication (Dhillon, Oki, Szyjka, Aparicio, & Kamakaka, 2006), DNA repair (Kalocsay, Hiller, & Jentsch, 2009), chromosome segregation and cohesion (Hou et al., 2010), chromatin and transcriptional regulation (Martins-Taylor, Sharma, Rozario, & Holmes, 2011; Papamichos-Chronakis, Watanabe, Rando, & Peterson, 2011).

Most H2A.Z functions directly relates to its specific localization in the genome. Upon DNA damage, H2A.Z is recruited to double stranded break sites to promote Rad53-mediated

DNA repair (Kalocsay et al., 2009). A genome-wide study describe H2A.Z's location primarily in the +1 nucleosome of Pol II promoters and it correlates with transcription silencing (Papamichos-Chronakis et al., 2011). Additionally, H2A.Z locates within the end of HM loci and telomere heterochromatin (Babiarz, Halley, & Rine, 2006; Meneghini, Wu, & Madhani, 2003). These characteristics define H2A.Z as a boundary element between heterochromatin and euchromatin. Interestingly, misslocalized H2A.Z has been correlated with genome instability and aneuploidy (Chambers et al., 2012; Papamichos-Chronakis et al., 2011), which shows the importance of correct regulation of H2A.Z genome-wide location.

The dynamic of H2A.Z within the genome is thought to be controlled by the NuA4 acetyltransferase complex and the chromatin remodeling complexes SWR1 and INO80 (Billon & Côté, 2013). The SWR1 complex recruits H2A.Z to chromatin by replacing the H2A-H2B dimer of the nucleosome for a H2A.Z-H2B pair. NuA4 stimulates SWR1's incorporation of H2A.Z by acetylation of the N-terminal lysine of histone H4 (K5, 8, 12 and 16) and H2A (K4, 7 and 13) to recruit Bdf1, a subunit of the SWR1 complex (Altaf et al., 2010). Conversely, the INO80 complex catalyzes the removal of H2A.Z-H2B dimer for the canonical counterpart (Altaf et al., 2010; Papamichos-Chronakis et al., 2011). Also, acetylation in H3K56 regulates H2A.Z's dynamics impairing SWR1 remodeling and increasing INO80's (Altaf et al., 2010). In contrast to INO80-mediated eviction, recent studies describe H2A.Z turnover as transcriptionally regulated (Jeronimo, Watanabe, Kaplan, Peterson, & Robert, 2015; Tramantano et al., 2016). Overall, the individual contribution of the INO80 complex to H2A.Z's dynamics, particularly in vivo, remains unclear.

## **Chromatin remodeling complexes**

Chromatin remodeling complexes are conserved multiprotein complexes that participate in the genome-wide dynamic maintenance of the chromatin. Interestingly, only a specific subset of subunits is conserved across eukaryotes, commonly subunits tightly related to molecular function. The remodeling occurs at the nucleosome level by acting through different mechanisms: eviction and insertion of nucleosomes to create accessible DNA, dimer exchange within a nucleosome and nucleosome sliding (Harikumar & Meshorer, 2015). Through these mechanisms, chromatin remodeling complexes regulate the nucleosome population and accessibility of DNA elements important for cellular processes such as promoters, origin of replications and enhancers. Due to its genome-wide chromatin regulation, remodelers regulate several cell processes including transcription, DNA replication, DNA repair and chromosome segregation (Clapier & Cairns, 2009; Harikumar & Meshorer, 2015; Morrison & Shen, 2009). Overall, these remodelers add another level of complexity to the dynamic regulation of chromatin structure besides histone composition, PTMs and histone variants.

The chromatin remodeling complexes are classified in four families: SWI/SNF, ISWI, CHD and INO80 families (Clapier & Cairns, 2009). All share common features that describe their function as remodelers, however the subunit quantities and composition vary between families. Primarily, remodelers hydrolyze ATP to catalyze the chromatin arrangement (Ryan & Owen-Hughes, 2011). Furthermore, chromatin remodeling complexes carry subunits to regulate the ATPase activity, recognition of PTM for targeted recruitment, varied nucleosome affinity and interaction with other chromatin proteins (Clapier & Cairns, 2009). The revision on chromatin remodeling within this work focuses on the INO80 complex and its role in genomic stability.

## The INO80 complex

The INO80 complex represents a conserved chromatin remodeling complex from the family of Snf2 proteins (Ryan & Owen-Hughes, 2011). Because of the multisubunit nature of the complex, the subunit composition varies, however specific subunits exhibit homology among distant species. Both human and budding yeast share common subunits: the catalytic subunit Ino80, two different copies of RuvB-like DNA helicases, Ies2, Ies6, monomeric Actin and three actin related proteins Arp4, Arp5 and Arp8. *Saccharomyces cerevisiae*'s INO80 complex is comprised of 15 different subunits: Ino80, Rvb1, Rvb2, Ies1-6, Act1, Arp4, Arp5, Arp8, Taf14 and Nhp10. Based on the cryo EM structure, the INO80 complex displays the Ino80 subunit as scaffold and describe 4 particular modules: a Rvb1/2 dodecamer, Arp5 module comprised by Arp5, Ies2 and Ies6, Nhp10 module constituted by Nhp10, Ies1, Ies3 and Ies5, and the Arp8 module formed Arp8, Arp4, Taf14, Act1 and Ies4 (Tosi et al., 2013). The assembly of these modules within the complex depends on interaction within the Ino80 subunit. The Ino80 subunit interacts with the Nhp10 module through the N-terminal tail and the Arp8 module through a HSA domain. The HSA domain represents the primary binding platform for the assemble of actin related proteins in chromatin remodeling complexes (Szerlong et al., 2008). The C-terminal contains a RecA1 and RecA2 domain, however the RecA2 presents an insertion responsible for the interaction with the Arp5 module and the Rvb1/2 dodecamer. Additionally, some of the subunits are shared with other complexes, Arp4 and Act1 coprecipitate with both NuA4 and SWR1 complexes and Rvb1/2 only with SWR1. Also, Arp5 and Ies6 forms a subcomplex of unknown additional functions in the cell (W. Yao et al., 2016). Additionally, Taf14 belongs to multiple complexes INO80, SWI/SNF, RSC, NuA3 histone acetylase and transcription initiation factors TFIIF and TFIID. Notably, the individual contributions of the subunits to INO80s

function require further research. Most studies have focused on the function of the conserved subunits.

Molecularly, the INO80 complex mediate nucleosome turnover, the exchange of the H2A.Z-H2B pair for H2A-H2B dimer and nucleosome sliding (Papamichos-Chronakis et al., 2011; Udugama, Sabri, & Bartholomew, 2011). Functionally, the INO80 complex participate in transcription, DNA replication, DNA repair, chromosome segregation and cell metabolism. INO80 regulates the genome-wide localization of H2A.Z primarily to +1 and TTS to delimitate silent chromatin (Xue et al., 2015). Similarly, deletion of subunits of the complex differentially affect gene expression (Papamichos-Chronakis et al., 2011; W. Yao et al., 2016). A recent study describes common regulation of cell functions among subunits as well as subunit exclusive functions (Beckwith et al., 2018). Both Arp8 and Arp5 exhibit similar genetic interactions, in contrast to the exclusive interaction of Ies6, suggesting variable contributions to the function of the complex despite the different structural module. Other phenotypes have been showed by deletion of subunits of the complex. Arp8 deletion mutants alter DNA replication, DNA repair and reduce Ino80's recruitment to chromatin (Lademann, Renkawitz, Pfander, & Jentsch, 2017; Shimada et al., 2008; W. Yao et al., 2016). In contrast to the variety of its functions, little is known about the regulation that affects the complex. In vitro studies show that inositol hexaphosphate inhibits the nucleosome sliding by the INO80 complex (Shen, Xiao, Ranallo, Wu, & Wu, 2003; Willhoft, Bythell-Douglas, McCormack, & Wigley, 2016). Also, the binding of the complex is mediated by H2A phosphorylation during DNA damage repair (Morrison et al., 2004).

The INO80 complex functions through the cell cycle, however the involvement in mitosis shows detrimental effects to the cell, particularly in chromosome segregation. In humans, both

overexpression and downregulation of Ino80 show regulation of diverse type of cancers (Poli, Gasser, & Papamichos-Chronakis, 2017). Similarly, disruption of the INO80 complex causes aneuploidy and structural abnormalities in the chromosome (Hur et al., 2010). Yeast mutants of subunits of the complex exhibit similar phenotypes; deletion of Ies6 increases ploidy and enriches H2A.Z in the pericentric region (Chambers et al., 2012) and deletion of Arp8 affects chromatin cohesion (Ogiwara, Enomoto, & Seki, 2007), suggesting a conserved role in chromosome segregation and chromosome structure. The INO80 complex controls the genomic location of the H2A.Z variant and euchromatin-associated PTMs. Deletion of the Ino80 subunit causes a mislocalization of H2A.Z in intragenic regions (Papamichos-Chronakis et al., 2011). Additionally, the INO80 complex controls the spread of H3K79me3 into intergenic regions (Xue et al., 2015). Similarly, deletion of Nhp10 suppresses the mislocalization of Cse4, suggesting that it might also control location of the centromeric H3 variant (Hildebrand & Biggins, 2016). Overall, the studies aforementioned suggest that the INO80 complex could participate in the control of pericentric chromatin by accurate localization of H2Z.A to prevent spreading of euchromatin and regulate centromere structure.

### **Chromosome segregation**

For accurate segregation of the chromosomes, the cells undergo a condensation of the chromosomes and bi-orientation to lead the chromosomes during the migration to the daughter cells. At the onset of mitosis, condensation is guided by the physical constraint of the chromatin fibers caused by cohesin and condensin (Antonin & Neumann, 2016). Additionally, PTMs mediate chromosome condensation mainly through H3T3 and H3S10 phosphorylation leading to H4K16 deacetylation. Previous to migration of the sister chromatids, the chromosomes exhibit a bidirectional orientation to guide the process. Bi-orientation requires the attachment of the sister

chromatid to the opposite spindle poles, through interaction of the microtubules, kinetochores and the centromere (Tanaka, Stark, & Tanaka, 2005). The spindle assembly checkpoint (SAC) arrests the cell by inhibiting the Anaphase Promoting Complex which cleaves cohesion and condensin presiding chromosome segregation (Krenn & Musacchio, 2015). SAC's function prevents the migration of incorrectly attached sister chromatid and promotes bi-orientation. Additionally, Aurora kinase B phosphorylates H3S10 and is primarily involved in the bi-orientation as well (Krenn & Musacchio, 2015). Similarly, Sgo1 regulates bi-orientation but unlike Aurora kinase B doesn't possess catalytic activity.

## **Sgo1**

Sgo1 was named “shugoshin” that means guardian spirit in Japanese for its role in conserving the correct segregation of chromosomes. Sgo1 maintains the correct segregation of chromosomes by regulating the bi-orientation of the sister chromatids (Wang & Dai, 2005). Failure in bi-orientation of the sister chromatids causes synthelic attachment between chromosomes and microtubules causing missegregation and chromosome loss. Sgo1 is highly conserved, however higher eukaryotes exhibit a homologue, Sgo2, with similar functions (Y. Yao & Dai, 2012). Particularly, Sgo1 associates with the heterochromatic pericentric region in fission yeast and humans (Yamagishi, Sakuno, Shimura, & Watanabe, 2008). Budding yeast also exhibits the pericentric location of Sgo1 despite of its highly gene-dense region around centromeres (Haase, Stephens, Verdaasdonk, Yeh, & Bloom, 2012). Bub1, a member of the SAC, appears to regulate the localization of Sgo1 in humans and yeast via phosphorylation of H2AS121 and H2AT120, respectively (Haase et al., 2012; Y. Yao & Dai, 2012). Notably, defective Sgo1 recruitment through H2A phosphorylation impairs kinetochore shape, microtubule dynamics and decreases bi-orientation of the chromosome. Mps1 has been shown to

regulate the spindle localization of Sgo1 and might mediate an interaction with the spindle assembly checkpoint (Storchová, Becker, Talarek, Kögelsberger, & Pellman, 2011). Together, these findings suggest that Sgo1 require precise localization to effectively regulate chromosome segregation

The regulatory mechanism of bi-orientation by Sgo1 remains unclear. However, the physical and genetic interactions of Sgo1 with other proteins reveal a hint on the regulatory pathways. Sgo1 overexpression suppresses benomyl sensitivity of histone mutants that causes impaired cell cycle progression, increased missegregation and monopolar chromosome attachment (S. Kawashima et al., 2011). This genetic interaction suggests that Sgo1 might regulate bi-orientation in altered chromatin that causes impaired chromosome segregation. Sgo1 interacts with Rst1, a subunit of the PP2A phosphatase, through a coiled-coil domain and recruits it to the pericentric region. Bi-orientation of chromosomes decreases in cell depleted of Rts1 in the pericentromere (Eshleman & Morgan, 2014). Additionally, Sgo1 recruits condensin and Ipl1 to the centromere, assisted by PP2A (Peplowska, Wallek, & Storchova, 2014). Overall, Sgo1 mediates the centromeric recruitment of proteins to regulate bi-orientation. However, the relationship between Sgo1 mediated bi-orientation and chromatin structure remain unexplored. This study explores the possible genetic interactions between INO80 and Sgo1 in the regulation of chromosome segregation.



### **III. METHODS**

### **A. *Saccharomyces cerevisiae* strains and media**

The *Saccharomyces cerevisiae* strains are listed in Table 1. The strains used for this study are isogenic to FY2, which originally derives from S288C, unless indicated otherwise (Winston, Dollard, & Ricupero-Hovasse, 1995). Most deletion mutants were obtained from the BY4741 deletion collection. Deletions of *INO80* and *IES3* were constructed by the PCR amplification product of GHB151 using the primer pairs oIP452/oIP453 and oIP470/oIP471, respectively and verified by the following primer pairs oIP451/oIP434 and oIP472/oIP434. Particularly, the *INO80* was deleted in JMx4-3B x FY1342 and sporulated to obtain the mutant in a haploid cell. The 13-Myc tag with Nat<sup>R</sup> as selectable marker was added to the C-terminal of *INO80* through recombination of the PCR product of plasmids pIP279 in the FY1342 strain. A list of primers is provided in Table 2.

The Yeast Extract Peptone Dextrose (YPD) was prepared as growth media for yeast strains. Synthetic dextrose minimal medium (SD), synthetic complete and dropout medium (SC) were prepared for selection of plasmid acquired strains and genotypic characterization of strains (Rose, 1990). Benomyl was added to hot YPD to reach concentrations of 10 and 15 µg/mL for sensitivity test of strains. Canavanine plates were prepared by adding canavanine sulfate to a final concentration of 3 µg/mL. For selection of deletion mutants, G-418 or hygromycin were added to YPD to concentrations of 200 µg/mL and 150 µg/mL, respectively.

### **B. *Escherichia coli* strains and media**

*E. coli* DH5 alpha cells were employed for amplification of plasmids. The *E. coli* strains carrying the plasmid were propagated in LB medium containing ampicillin at 100 µg/mL.

### C. Design of 13-Myc plasmid with Nat<sup>R</sup> marker

The 13-Myc plasmid with Nat<sup>R</sup> marker was constructed by replacement of the KanMX6 marker of plasmid GHB160 by the Nat<sup>R</sup> cassette of pAG25. GHB160 was digested with PmeI and BglII in their respective cutting buffers, the DNA was separated in a 0,8 % agarose gel and the 13-Myc vector gel extracted. pAG25 was digested with EcoRV and BglII, the Nat<sup>R</sup> cassette separated and extracted as mentioned previously. The Nat<sup>R</sup> cassette was cloned in the 13-Myc vector with T4 ligase and incubation overnight at room temperature. Competent DH5 alpha *E.coli* were transformed with the ligation product using standard procedures (Sambrook J., 1989). The resulting plasmid was named pIP279. The plasmids used in this study are summarized in Table 3.

### D. Double mutant construction

The double mutant strains carrying deletion of *SGO1* and subunits of the INO80 complex were generated after multiple crossing and transformation. Crossing of IPY1109 and FY1333 generated a *SGO1* heterozygous diploid and sporulation of the diploid produced JGx2-1C, haploid strain with *SGO1* deleted. JGx2-1C was crossed with BY4741 to generate another haploid *sgo1Δ* mutant strain, JMx4-3B. Finally, JMx4-3B x FY1342 was generated by mating JMx4-3B and FY1342 and transformed to delete genes *ARP5*, *ARP8*, *TAF14* and *INO80* of the INO80 complex. The genes were deleted by recombination with the marker cassettes using the Gietz Lithium Transformation procedure (Gietz & Schiestl, 2007; Gietz, Schiestl, Willems, & Woods, 1995). Additionally, the double mutant diploids were transformed with either the *SGO1* high copy plasmid pIP153 or the vector YEplac181. The diploids carrying the double deletions alone and with the plasmids were sporulated to obtain the respective double mutant haploids.

### **E. Benomyl sensitivity assay**

Cells were grown up to approximately  $10^8$  cell/mL and counted with a hemocytometer. The concentration of cells was adjusted to  $10^8$  cell/mL and diluted serially 10-fold to down to  $10^3$  cell/mL. Of each dilution 5  $\mu$ L were linearly spotted on YPD and YPD + benomyl at 10 and 15  $\mu$ g/mL and incubated at 30 °C for 3 to 5 days. The sensitivity was assessed by impaired growth in benomyl plates.

### **F. Canavanine assay of ploidy**

Cells were streaked on YPD plates and grown for 2 days, followed by replica plating on SC-Arg and SC-Arg + canavanine and mutagenized by UV light (300 ergs/mm<sup>2</sup>). Plates were incubated in the dark at 30 °C for 3 to 4 days. Ploidy was assessed by cell growth. Appearance of papillae indicated haploid strains due to mutagenesis of the single copy of *CAN1* gene. However, diploid mutants won't grow because of the uptake and toxicity of canavanine by a second unmutated copy of the *CAN1* permease gene.

### **G. Flow cytometry**

Cells were exponentially grown in YPD, pelleted and later fixed in a mixed solution comprised of 300 $\mu$ L of 50 mM Tris pH 7.5 and 700 $\mu$ L ethanol 95%. Cells were pelleted and washed with 50mM Tris pH 7.5. Subsequently, the washed cells were resuspended in 100  $\mu$ L 50 mM Tris pH 7.5 treated with RNase at 1 mg/mL and incubated at 37 °C overnight. Next, 5  $\mu$ L Proteinase K (20 mg/mL) was added and incubated at 50 °C for 1 hour. The cells were stained with a solution of propidium iodide diluted at 15  $\mu$ g/mL in 50mM Tris pH 7.5 buffer and sonicated for 5 seconds in Branson 1510 sonicator. Stained cells were kept at 4 °C in the dark

until flow cytometry analysis in (BD Biosciences). Results are reported by recording a minimum of 10 000 events.

#### **H. Chromatin Immunoprecipitation assay**

Chromatin immunoprecipitation (ChIP) was carried out in a wild type untagged strain, INO80-13Myc tagged and *arp8Δ* with INO80-13Myc tagged strains. The antibody employed was anti-c-Myc (Roche, 9E10) and protein G Dynabeads for immunoprecipitation (Invitrogen-ThermoFisher) The ChIP was performed according to standard method (Kanta, Laprade, Almutairi, & Pinto, 2006). The pericentromeric location was assessed by PCR with the primer pair oIP210/oIP211 for the 0,5 Kb left flanking region of *CEN3*. The PCR product was resolved in a 1.0 % agarose gel with ethidium bromide and imaged in a FluorChem™ 8900 instrument (Alpha Innotech).

## **IV. RESULTS**

## Specific subunits of complexes INO80 and SWR1 affect ploidy

The deletion mutants of the subunits of the INO80, SWR1, NuA4 and the *HTZ1* gene were obtained from the BY4741 deletion collection, unless indicated otherwise. For the INO80 complex, the subunits investigated were Ino80, Ies1 to Ies6, Taf14, Nhp10, Arp4, Arp5, Arp8. *ARP4* is an essential gene, therefore the subunit Arp5 was assessed in the temperature sensitive mutant *arp4-26*. The subunits Swr1, Swc2-7, Bdf1, Yaf9 and Arp6 of the SWR1 complex were also analyzed, as well as the Eaf1, Eaf3, Eaf6 and Eaf7 corresponding to the NuA4 complex. The deletion of *INO80* and *IES3* were obtained by targeted transformation and recombination. The purpose of the analysis was to identify the key subunits of these complexes related to chromosome segregation, primarily focused in the ploidy maintenance. The ploidy status of the mutants was initially analyzed by performing a canavanine assay, which monitors the copy number of chromosome V. The results of the canavanine assay are shown in Figure 1. Overall, a small number of subunits of the complexes caused increased ploidy in the cell. The deletion mutants of *ARP5*, *IES6*, *ARP8* and *TAF14* of the INO80 complex showed increased ploidy. Regarding SWR1 complex the diploid causing mutants were *swr1Δ*, *bdf1Δ*, *yaf9Δ*, and *swc5Δ*. Although *swc6Δ* showed some papillae indicative of a haploid state, the amount was lower compared to the haploid control, and flow cytometry analysis (see below) confirmed that it had diploidized. Notably, deletion of *HTZ1* doesn't affect ploidy. None of the NuA4 exclusive subunits assessed affected ploidy, however these don't comprise the entire subunit composition of the complex and the remaining subunits remain to be explored.

Flow cytometry of the mutants was performed for a more accurate assessment of ploidy in the mutants. Flow cytometry provides a better measurement of ploidy by considering the size of the cell and the whole DNA content of the cell compared to the canavanine test that evaluates

ploidy based on the copy of chromosome V. Figure 2 shows the results of the flow cytometry analysis of the subunits of the INO80 complex. In addition to the mutants analyzed by the canavanine assay, the *arp4-26* and *ino80Δ* mutants were included in flow cytometry analysis. Overall, the flow cytometry analysis confirmed the ploidy increased showed in the canavanine assay for subunits of the INO80 complex. In the *ino80Δ* mutant it can be observed a mixed population of haploid and diploid cells, due to the short time of growth after germination. Additionally, the temperature sensitive mutant *arp4-26* increased ploidy only under growth at 37 °C, but remained haploid at 26 and 30 °C. This subunit is shared among the three complex and might indicate a common mechanism of action.

As shown in Figure 3, *swr1Δ*, *bdf1Δ*, *yaf9Δ*, and *swc6Δ*, increased ploidy in support of the canavanine data, however *swc5Δ* exhibited both haploid and diploid phenotype. The inconsistency of the phenotypes of *swc5Δ* and *swc6Δ* in both ploidy assays suggest that these mutants undergo increased ploidy later than the other mutants of the complex and perhaps less relevant contribution to genomic maintenance. The DNA content of the mutants of the NuA4 complex and *htz1Δ* confirms the haploid phenotype observed in the canavanine assay.

### **Ploidy increase correlates with benomyl sensitivity**

The benomyl sensitivity test correlates well with mutations that impair chromosome segregation. Benomyl destabilizes the polymerization of microtubules increasing failure in microtubule attachment and tension; causing missegregation of chromosomes. Results of benomyl sensitivity test are shown in Figure 4. Only subunits of the INO80 and SWR1 complexes were assessed; NuA4 was excluded from the rest of the study. The deletion of *Ies6*, *Arp5*, *Taf14* and *Arp8* of INO80 complex increased the sensitivity to benomyl, correlating with the ploidy analysis. Within the SWR1 complex, *swr1Δ*, *bdf1Δ*, *yaf9Δ*, *swc2Δ*, *swc3Δ*, *swc5Δ*,



*swc6Δ* and *swc7Δ* increased sensitivity to benomyl. Interestingly, some benomyl sensitive mutants of SWR1 complex (*swc2Δ*, *swc3Δ* and *swc7Δ*) don't diploidize. Table 4 summarizes the correlation between benomyl sensitivity and ploidy increase. This suggests that mutations in specific subunits of the complex govern the maintenance of segregation and other subunits provide a supplementary effect on the function of the complex, but still affecting tension or microtubule attachment problems. Notably, *htz1Δ* showed a high sensitivity to benomyl, however remained haploid. Since both INO80 and SWR1 complexes have H2A.Z as a substrate (Gerhold & Gasser, 2014; Morrison & Shen, 2009), the increased ploidy phenotypes of these complexes can't be explained by absence of H2A.Z in the chromatin.

### **Interaction of the INO80 complex with *SGO1***

Overexpression of *SGO1* has been shown to suppresses the sensitivity to benomyl and alleviate chromosome missegregation (S. Kawashima et al., 2011). The analyzed interactions with *SGO1* were focused on the ploidy increase mutants of the INO80 complex. Mutants of subunits that are exclusive to the INO80 complex were transformed with either plasmid YEplac181 as vector control or plasmid pIP153 to allow high copy expression of *SGO1*. The transformed mutants were grown overnight between 1 to 2 days in selective medium (SC-Leu) to maintain the plasmids. The saturated culture was adjusted to  $1 \times 10^8$  cell/mL and diluted for benomyl sensitivity assay (Methods). Subunits exclusive to INO80 were selected to avoid ambiguous phenotypes due to possible additive or synergistic effects of multi-complex subunits. For this analysis, mutants of the BY4741 deletion collection were evaluated. The *taf14Δ* mutant was excluded of the analysis because it belongs to multiple complexes including: TFIID, TFIIF, NuA3, SWI/SNF and INO80. Of the exclusive mutants, *arp5Δ* and *arp8Δ* were selected, *ies6Δ*

was excluded because of reports suggesting stability dependent of Arp5 and both forming a subcomplex (W. Yao et al., 2015; W. Yao et al., 2016).

Surprisingly, overexpression of *SGO1* caused different phenotypes in members of the same complex. High copy of *SGO1* exacerbated the benomyl sensitivity of an *arp8Δ* mutant, suggesting an increased missegregation. In contrast, the overexpression of *SGO1* didn't affect the sensitivity in *arp5Δ*. This difference in phenotype towards *SGO1* overexpression suggests different genetic interactions of subunit despite of belonging to a same complex. Additionally, these findings attribute different functional properties to specific subunits or even the structural modules of the complex. Importantly, the mutants used in the transformation were already diploid. The effect observed in the experiment might not reflect any protective or disruptive effects of *SGO1* before diploidization.

The strain JMx4-3B x FY1342 was prepared to obtain a diploid heterozygous for *sgo1Δ* and further delete subunits of INO80. The subunits selected for deletion were Ino80, Arp5, Arp8, Taf14, Ies3 and Ies4 to evaluate the phenotypes of the double mutants. After transformation with specific deletion-PCR product for the targeted gene and verification of the deleted gene, the diploid was sporulated and the segregants with double mutants were selected for analysis. In general, the double mutants experienced poor germination, rarely producing growth on 4 spores of the dissected tetrads, particularly in the increase in ploidy mutants of INO80. Interestingly, the *ino80Δsgo1Δ* and *arp5Δsgo1Δ* double mutants couldn't be obtained after germination of the tetrads. The remaining double mutants were analyzed through benomyl sensitivity assay.

The double mutants analyzed for benomyl sensitivity were *arp8Δsgo1Δ*, *ies3Δsgo1Δ*, *ies4Δsgo1Δ* and *taf14Δsgo1Δ*. Three different double mutant and corresponding single mutant segregants were analyzed and compared with both parental strains. Overall, the *sgo1Δ* single

mutants showed similar sensitivity to the JMx4-3B parent with deleted *SGO1* (Figure 6). The *arp8Δ*, *ies3Δ*, *ies4Δ* and *taf14Δ* mutants segregated from the diploid exhibited similar sensitivities those seen in Figure 4, showing consistency of the phenotype despite the difference in strains. Notably, all double mutants exhibited lower growth on YPD compared to the wild-type parent FY1342, yet similar to JMx4-3B indicating similar growth defect to the *SGO1* deletion. Additionally, the double mutants were more sensitive than the corresponding single subunit mutant of INO80, however similar to *sgo1Δ*. These results suggest that deletion of INO80's subunits don't affect *sgo1Δ*'s sensitivity and might be in similar pathways in regard to microtubule tension and attachment. By comparing Figure 3 and 4B, benomyl sensitivity test don't always reflect the increased ploidy phenotype and flow cytometry is required for a clearer assessment of the double mutants in chromosome segregation.

The DNA content of the double mutants showed no effect in the ploidy state of the *ies3Δsgo1Δ*, *ies4Δsgo1Δ* (Figure 7). Contrary to the results showed in Figure 2., the newly germinated *arp8Δ* mutant showed haploid profile. Additionally, different segregants of the heterozygous double mutant *arp8Δsgo1Δ* exhibit both haploid and diploid ploidy states. The presence of the haploid state on both *arp8Δ* and *arp8Δsgo1Δ* suggest that these haploid mutants require further cell divisions for complete diploidization. Also, it can't be determined if deletion of *SGO1* contributed to diploidization of one of the segregants, for further inspection the number of generations should be accounted. In contrast, both *taf14Δ* and *taf14Δsgo1Δ* consistently exhibited the increased ploidy phenotype. It remains unclear if the double mutation contributed to further increase of ploidy or a faster diploidization compare to the single mutant. Overall, the double deletions didn't show clear interaction in ploidy between these subunits of INO80 and Sgo1.

## Overexpression of *SGO1* suppresses chromosome instability of specific mutants of INO80

Heterozygous diploid strains of *arp5Δ sgo1Δ* and *ino80Δ sgo1Δ* were transformed with plasmids YEPlac181 and pIP153 to further sporulate and select the *arp5Δ* and *ino80Δ* segregants that retained the plasmid after germination. The *arp8Δ sgo1Δ* was transformed as well with both plasmids but the *arp8Δ* mutant with pIP153 wasn't obtained after several dissections.

Additionally, the *arp8Δ sgo1Δ* diploid experienced poor retention of the pIP153 plasmid after germination, although this was only a qualitative observation. The overexpression of *SGO1* suppressed the benomyl sensitivity of the *arp5Δ* and *ino80Δ* strains, being the suppression greater for *ino80Δ sgo1Δ* (Figure 8). The increased resistance to benomyl by overexpression of *SGO1* suggests a decrease in chromosome missegregation. However, this test doesn't allow to verify if the overexpression protects against diploidization.

The *ino80Δ* segregants of the heterozygous diploid of *ino80Δ sgo1Δ* that retained the plasmids were grown to mid-log in selective medium for the maintenance of the plasmids, fixed and their DNA content analyzed by flow cytometry. The *ino80Δ* mutant exhibited haploid and diploid profiles in different segregants containing the vector, but stayed haploid by keeping the high copy plasmid with *SGO1* (Figure 9). The profile of the haploid *ino80Δ* with the vector suggests that the mutant is in process of diploidization. These preliminary results of DNA content suggest that overexpression of *SGO1* suppresses the increase in ploidy phenotype of *ino80Δ*. However, further analysis is required to determine if the overexpression of *SGO1* is sufficient for protection from ploidy increase or only delays the process.

## **Loss of Arp8 doesn't affect pericentromeric binding of Ino80**

A past study showed that the INO80 complex can locate in specific regions throughout the genome (Papamichos-Chronakis et al., 2011). Due to the importance of the centromere in chromosome segregation, we decided to explore if the INO80 complex locates in the periphery of the centromere (pericentromere). Additionally, we wanted to determine if the loss of Arp8 could cause decrease of binding to the genome. As shown in Figure 10, Ino80 locates within 0.5 Kb to the left from centromere III. Additionally, the loss of Arp8 doesn't affect the binding of Ino80 in this region. Additional ChIP experiments in flanking regions of the centromere are required to describe if the pericentromeric location of INO80 is universal across all centromeres. Additionally, Ino80 have been shown to increase binding to chromosomal regions during cell cycle arrest which suggest that the complex might have differential binding throughout the cell cycle (Shimada et al., 2008). Overall, pericentromeric localization of Ino80 is not affected by ARP8 deletion, indicating that the recruitment of the complex to this region depends on other subunits.

## **V. DISCUSSION**

## Specific subunits of INO80 and SWR1 involved in chromosome segregation

The functional significance of the diverse subunit composition of INO80, SWR1 and NuA4 complexes remains unknown. It is important to determine the influence of the structure of these complexes to better understand their function and regulations. Due to structural complexity, the study of these complexes represents a big challenge to assess the relevance of each subunit in the function of a given complex. Additionally, these complexes share subunits that might contribute to a common mechanism of action. This study analyses the effects of specific subunits of each complex in maintaining chromosome segregation and then focuses on the involvement of the INO80 complex by further exploring the contribution of its subunits in more detail. Initially, the results demonstrate that the absence of specific subunits cause ploidy increase. For the INO80 complex, deletion of *INO80*, *ARP5*, *ARP8*, *IES6* and *TAF14* causes ploidy increase. Similarly, mutants of *SWR1*, *YAF9*, *BDF1*, *SWC5* and *SWC6* diploidized the cell. Additionally, the temperature sensitive mutant of the shared subunit Arp4 increased ploidy at 37 °C. The results suggest similarities as well as differences regarding to the function of the complexes. Deletion of Ino80 and Swr1, the scaffold protein of each complex, suggests that the complex requires an assembly agent to maintain proper function in chromosome segregation. The *arp4-26* mutant causing increased ploidy at non-permissive temperature could indicate a similar mechanism of function. Particularly, *arp4-26* contains a single mutation of G187R, located outside of the binding pocket of ATP. Figure 11 shows the ribbon model of Arp4 based on crystallographic data and indicates the location of the G187R mutation with respect to the ATP binding site. Crystallographic analysis suggests that ATP binds tightly to Arp4 and is involved in the folding of the protein (Fenn et al., 2011), suggesting that the G187R mutation of

*arp4-26* causes poor ATP binding and improper folding at the restricted conditions. Therefore, the presence of Arp4 appears essential for the maintenance of normal ploidy.

### **Analysis of subunit contribution to the INO80 complex in chromosome segregation**

The single deletion of subunits of INO80 allows the assessment the importance of each member in the function of the complex, by testing for different phenotypes. Similarly, the physical interactions between the subunits add a mechanistic connection to the phenotype, by examining the integrity of the complex in those mutants. The reports of this study indicate that mutants of *INO80*, *ARP4*, *ARP5*, *ARP8*, *IES6* and *TAF14* increase ploidy and increase sensitivity to benomyl. This suggests that the deletion of these subunits perturb the chromatin remodeling function of the complex and leads to chromosome instability. In contrast, the absence of the *Ies1*, *Ies2*, *Ies3*, *Ies4*, *Ies5* and *Nhp10* doesn't affect chromosome segregation. These subunits may be required for assembly, stability, or recruitment of the complex related to other functions, such as DNA repair or transcription, but not essential for the role of INO80 complex in chromosome segregation. Recent structural studies describe the complex in specific modules due to the importance in the integrity of the complex (Tosi et al., 2013). The deletion of *INO80* causes the loss of the main scaffold for the full assembly of the complex. The loss of specific physical interaction between the subunits has been shown to cause partial assembly of the complex and could affect biochemical and biological functions. The deletion of *ARP8* causes full loss of Arp4, *Ies4* and partial loss of Act1 and Taf14 in pull down experiments. This arrangement of subunit interactions suggests that phenotypes observed for chromosome segregation might involve the combine action of the subunits physically interacting with Arp8. Similarly, loss of Taf14 through deletion diploidized the cell, however the cause of this phenotype could be indirect since Taf14 is also found in other cellular complexes. Finally, Arp5 and *Ies6* belong to another module and



their deletion also increased ploidy, indicating than more than one module is involved in maintaining the function of INO80. Within this study, *ARP5* was selected for further analysis of the complex in chromosome segregation due to previous studies indicating this subunit as requirement for stability of Ies6. Interestingly, *INO80*, *ARP8*, *ARP5* and *IES6* are also conserved in humans. Ultimately, these structural units of the complex represent key structural elements for maintenance of the function of the complex and correct chromosome segregation.

The phenotypic assessment and subunit composition of the INO80 complex highlights the importance of actin and acting related proteins (Arps) in its function. Commonly, actin exists as filamentous actin (F-actin) and globular actin (G-actin). Interestingly, Act1, Arp4, Arp5 and Arp8 appear as monomers within the INO80 complex. The presence of the structural similarities of these proteins along the complex suggests that these subunits might contribute mainly to structural integrity of the complex and therefore could be affecting chromosome segregation. However, our results indicate that Arp8 and Arp5 contribute differently in chromosome segregation due to the different genetic interaction with *SGO1* (Figures 5, 6 and 8). Therefore, in spite of their homology it appears that Arp5 and Arp8 have different functions within the complex. Additionally, Act1 and Arp4 belong to multiple complexes and might be involved in a general structural feature of chromatin remodeling complexes.

The ATPase activity of the complex represents the primary energy supply for the DNA translocation that leads to chromatin remodeling. Structural analysis of Arp4 and Arp8 indicate that both have ATP-binding sites, yet there haven't been reports of ATPase activity (Fenn et al., 2011). With the current information, Ino80 represents the primarily subunit of the complex responsible for ATP hydrolysis. However, Arp8 and Arp5 modulate the ATPase activity of the complex in the presence of nucleosomes (Tosi et al., 2013). Deletion of both subunits decreases

the affinity of the complex for the nucleosome and the remodeling activity (Shen, Ranallo, Choi, & Wu, 2003; Tosi et al., 2013; W. Yao et al., 2016). Our results indicate different contributions from Arp8 and Arp5 to chromosome segregation (Figure 5, 6 and 8). Since these reports describe in vitro conditions, the difference of Arp8 and Arp5 might be related to the biological function of the complex.

### **Differential genetic interaction of *ARP5* and *ARP8* with *SGO1* relevant to chromosome segregation**

The function of the INO80 complex is to remodel chromatin, specifically the exchange of H2A.Z-H2B dimers by H2A-H2B. The histone exchange accomplished by this complex impacts several biological functions and processes. The loss of INO80 causes a global mislocalization of nucleosomes throughout the genome (Papamichos-Chronakis et al., 2011). As mentioned before, *INO80*, *ARP4*, *ARP5*, *ARP8*, *IES6* and *TAF14* contribute to the maintenance of INO80's function and keep chromosomal stability (Figures 1, 2 and 4). The correlation between ploidy increase and benomyl sensitivity of these subunits (Table 4) indicates that the impairment of INO80's function causes errors in microtubule attachment that leads to missegregation of chromosomes and diploidization. Sgo1 protects the chromosomes from missegregation by promoting bi-orientation. Based on this function, overexpression of *SGO1* could alleviate the missegregation phenotype of the mutants of the INO80 complex. Overexpressed *SGO1* had no effect on *arp5Δ* but increases benomyl sensitivity of *arp8Δ*. Based on this observation, we believe that *SGO1* in high copy won't reverse the sensitivity of these mutants that were already diploid before the introduction of the plasmid. Considering these different phenotypes of *ARP5* and *ARP8*, each might interact differently with *SGO1*. After multiple germinations, the *arp8Δ* mutant germinated with the pIP153 plasmid was not found, further analyses are required to determine if the

overexpression of *SGO1* is lethal to newly germinated *arp8Δ* mutants. As shown by our results, *SGO1* overexpression suppresses the sensitivity to benomyl of the *arp5Δ* mutant germinated with the high copy plasmid (Figure 8). The current reports of *arp5Δ* mutants suggest that the Arp5-Ies6 module get recruited to the insertion region of Ino80 and mediate the ATP activity of the complex (Tosi et al., 2013; W. Yao et al., 2016). The ATP hydrolysis of the complex represents a later stage on the mechanism of chromatin remodeling and relates to the binding of Arp5-Ies6 to the final step on the assembly of the complex. Conversely, conformational changes of a fully assembled complex might also trigger the ATP hydrolysis. Ultimately, loss of Arp5 interferes with the remodeling activity by reducing the efficiency of ATP hydrolysis of the complex; likely resulting in the chromosome missegregation phenotype.

Overexpression of *SGO1* suppresses both benomyl sensitivity and increase in ploidy of *ino80Δ* mutants (Figure 8 and 9). Deletion of *INO80* commonly shows the most deleterious phenotypes among the rest of the subunits (Papamichos-Chronakis et al., 2011). The loss of the scaffold and ATPase properties of the INO80 complex represents the most extreme impairment of its function. Interestingly, by overexpressing *SGO1* yeast cells can partially overcome the lack of function of the INO80 complex, suggesting that the defects in chromosomes segregation caused by deletion of *INO80* can be fixed by correcting chromosomal bi-orientation.

### **INO80 conserves pericentromeric binding upon *ARP8* deletion**

We further analyzed the presence of Ino80 in the flanking region of the centromere. The ChIP experiment demonstrated that Arp8 doesn't affect the binding of Ino80 to the centromere (Figure 10). This indicates that the increase in ploidy phenotype of *arp8Δ* is not related to recruitment of the complex to the pericentromeric region. The increased ploidy might be caused by the inability of the complex to remodel chromatin in the absence of Arp8 due to the lower

ATPase activity. The crosslink profile of the subunits of the complex suggest that Arp4 might interact directly with the HSA domain of Ino80 (Tosi et al., 2013). This domain is also present in Swr1 and has been recently shown to interact directly with a Act1-Arp4 dimer (T. Cao et al., 2016). Figure 12 shows the tertiary complex between the HSA domain of Swr1, Act1 and Arp4 based on crystallography data. These finding stress the relevance of Act1 and Arp4 in the assembly of the complex. Our ChIP analysis suggests that a partially assembled INO80 complex remains bound in the pericentromeric region of the genome but not fully functional, since Ino80 is still present in the absence of Arp8. This stalled INO80 complex might be the cause of enrichment of H2A.Z in the pericentromeric region and result in chromosome missegregation. Consistently, deletion of *IES6* has been shown to enrich H2A.Z in the pericentromeric region (Chambers et al., 2012). Further analysis of H2A.Z levels in INO80 mutants studied here will be required to validate this hypothesis. Since the regulations of chromosome segregation mainly occurs during mitosis, further studies are required to determine if the increase in ploidy phenotype of the INO80 mutants is related specifically to mitosis or a general effect throughout the cell cycle.

The levels of histones H2A and H2A.Z at centromeric regions may vary throughout the cell cycle. The function of the INO80 complex might become relevant during mitosis to remove H2A.Z from the pericentromeric region. H2A.Z lacks the phosphorylation site (S121) of H2A responsible for recruitment of Sgo1 in yeast which suggests that enrichment of H2A.Z caused by impairment of INO80 function might affect pericentromeric location of Sgo1, and perhaps other kinetochore-associated proteins.

**Table 1.** Yeast strains use in the study

Strain or identification	Lab name	Description
BY4741		<i>MATa his3Δ1 leu2Δ0 met15Δ0 ura3Δ0</i>
BY4741 <i>ies1Δ</i>		<i>MATa his3Δ1 leu2Δ0 met15Δ0 ura3Δ0 ies1Δ::KanMX</i>
BY4741 <i>ies2Δ</i>		<i>MATa his3Δ1 leu2Δ0 met15Δ0 ura3Δ0 ies2Δ::KanMX</i>
BY4741 <i>ies3Δ</i>		<i>MATa his3Δ1 leu2Δ0 met15Δ0 ura3Δ0 ies3Δ::KanMX</i>
BY4741 <i>ies4Δ</i>		<i>MATa his3Δ1 leu2Δ0 met15Δ0 ura3Δ0 ies4Δ::KanMX</i>
BY4741 <i>ies5Δ</i>		<i>MATa his3Δ1 leu2Δ0 met15Δ0 ura3Δ0 ies5Δ::KanMX</i>
BY4741 <i>ies6Δ</i>		<i>MATa his3Δ1 leu2Δ0 met15Δ0 ura3Δ0 ies6Δ::KanMX</i>
BY4741 <i>arp5Δ</i>		<i>MATa his3Δ1 leu2Δ0 met15Δ0 ura3Δ0 arp5Δ::KanMX</i>
BY4741 <i>arp8Δ</i>		<i>MATa his3Δ1 leu2Δ0 met15Δ0 ura3Δ0 arp8Δ::KanMX</i>
BY4741 <i>nhp10Δ</i>		<i>MATa his3Δ1 leu2Δ0 met15Δ0 ura3Δ0 nhp10Δ::KanMX</i>
BY4741 <i>taf14Δ</i>		<i>MATa his3Δ1 leu2Δ0 met15Δ0 ura3Δ0 taf14Δ::KanMX</i>
BY4741 <i>bdf1Δ</i>		<i>MATa his3Δ1 leu2Δ0 met15Δ0 ura3Δ0 bdf1Δ::KanMX</i>
BY4741 <i>arp6Δ</i>		<i>MATa his3Δ1 leu2Δ0 met15Δ0 ura3Δ0 arp6Δ::KanMX</i>
BY4741 <i>swr1Δ</i>		<i>MATa his3Δ1 leu2Δ0 met15Δ0 ura3Δ0 swr1Δ::KanMX</i>

**Table 1. (Cont.)**

Strain or identification	Lab name	Description
BY4741 <i>yaf9Δ</i>		<i>MATa his3Δ1 leu2Δ0 met15Δ0 ura3Δ0 yaf9Δ::KanMX</i>
BY4741 <i>swc2Δ</i>		<i>MATa his3Δ1 leu2Δ0 met15Δ0 ura3Δ0 swc2Δ::KanMX</i>
BY4741 <i>swc3Δ</i>		<i>MATa his3Δ1 leu2Δ0 met15Δ0 ura3Δ0 swc3Δ::KanMX</i>
BY4741 <i>swc5Δ</i>		<i>MATa his3Δ1 leu2Δ0 met15Δ0 ura3Δ0 swc5Δ::KanMX</i>
BY4741 <i>swc6Δ</i>		<i>MATa his3Δ1 leu2Δ0 met15Δ0 ura3Δ0 swc6Δ::KanMX</i>
BY4741 <i>swc7Δ</i>		<i>MATa his3Δ1 leu2Δ0 met15Δ0 ura3Δ0 swc7Δ::KanMX</i>
BY4741 <i>htz1Δ</i>		<i>MATa his3Δ1 leu2Δ0 met15Δ0 ura3Δ0 htz1Δ::KanMX</i>
BY4741 <i>eaf1Δ</i>		<i>MATa his3Δ1 leu2Δ0 met15Δ0 ura3Δ0 eaf1Δ::KanMX</i>
BY4741 <i>eaf3Δ</i>		<i>MATa his3Δ1 leu2Δ0 met15Δ0 ura3Δ0 eaf3Δ::KanMX</i>
BY4741 <i>eaf6Δ</i>		<i>MATa his3Δ1 leu2Δ0 met15Δ0 ura3Δ0 eaf6Δ::KanMX</i>
BY4741 <i>eaf7Δ</i>		<i>MATa his3Δ1 leu2Δ0 met15Δ0 ura3Δ0 eaf7Δ::KanMX</i>
FY1333		<i>MATa leu2Δ0 ura3Δ0</i>
FY1342		<i>MATa leu2Δ0 met15Δ0 ura3Δ0</i>
	IPY812	
	IPY1109	
JGx2-1C		<i>MATa leu2<sup>-</sup> lys2Δ202 ura3<sup>-</sup> sgo1Δ::HphMX</i>
JMx4-3B		<i>MATa leu2<sup>-</sup> lys2Δ202 ura3<sup>-</sup> sgo1Δ::HphMX</i>

**Table 1. (Cont.)**

Strain or identification	Lab name	Description
JMx4-3B x FY1342		<i>MATa/α leu2Δ0/ leu2<sup>-</sup> lys2Δ202/LYS2 met15Δ0/MET15 ura3Δ0/ ura3<sup>-</sup> SGO1/ sgo1Δ::HphMX</i>
JMx13		<i>MATa/α leu2Δ0/ leu2<sup>-</sup> lys2Δ202/LYS2 met15Δ0/MET15 ura3Δ0/ ura3<sup>-</sup> IES4/ ies4Δ::KanMX SGO1/ sgo1Δ::HphMX</i>
JMx14	IPY1206	<i>MATa/α leu2Δ0/ leu2<sup>-</sup> lys2Δ202/LYS2 met15Δ0/MET15 ura3Δ0/ ura3<sup>-</sup> ARP8/ arp8Δ::KanMX SGO1/ sgo1Δ::HphMX</i>
JMx15	IPY1209	<i>MATa/α leu2Δ0/ leu2<sup>-</sup> lys2Δ202/LYS2 met15Δ0/MET15 ura3Δ0/ ura3<sup>-</sup> TAF14/ taf14Δ::KanMX SGO1/ sgo1Δ::HphMX</i>
JMx16	IPY1207	<i>MATa/α leu2Δ0/ leu2<sup>-</sup> lys2Δ202/LYS2 met15Δ0/MET15 ura3Δ0/ ura3<sup>-</sup> ARP5/ arp5Δ::KanMX SGO1/ sgo1Δ::HphMX</i>
JMx17	IPY1205	<i>MATa/α leu2Δ0/ leu2<sup>-</sup> lys2Δ202/LYS2 met15Δ0/MET15 ura3Δ0/ ura3<sup>-</sup> INO80/ ino80Δ::KanMX SGO1/ sgo1Δ::HphMX</i>
JMx18		<i>MATa/α leu2Δ0/ leu2<sup>-</sup> lys2Δ202/LYS2 met15Δ0/MET15 ura3Δ0/ ura3<sup>-</sup> IES3/ ies3Δ::KanMX SGO1/ sgo1Δ::HphMX</i>
JMx19		<i>MATa/α leu2Δ0/ leu2<sup>-</sup> lys2Δ202/LYS2 met15Δ0/MET15 ura3Δ0/ ura3<sup>-</sup> SGO1/ sgo1Δ::HphMX &lt;YEplac181&gt;</i>
JMx20		<i>MATa/α leu2Δ0/ leu2<sup>-</sup> lys2Δ202/LYS2 met15Δ0/MET15 ura3Δ0/ ura3<sup>-</sup> SGO1/ sgo1Δ::HphMX &lt;pIP153&gt;</i>
JMx21		<i>MATa/α leu2Δ0/ leu2<sup>-</sup> lys2Δ202/LYS2 met15Δ0/MET15 ura3Δ0/ ura3<sup>-</sup> ARP8/ arp8Δ::KanMX SGO1/ sgo1Δ::HphMX &lt;YEplac181&gt;</i>
JMx22		<i>MATa/α leu2Δ0/ leu2<sup>-</sup> lys2Δ202/LYS2 met15Δ0/MET15 ura3Δ0/ ura3<sup>-</sup> ARP8/ arp8Δ::KanMX SGO1/ sgo1Δ::HphMX &lt;pIP153&gt;</i>
JMx23		<i>MATa/α leu2Δ0/ leu2<sup>-</sup> lys2Δ202/LYS2 met15Δ0/MET15 ura3Δ0/ ura3<sup>-</sup> TAF14/ taf14Δ::KanMX SGO1/ sgo1Δ::HphMX &lt;YEplac181&gt;</i>
JMx24		<i>MATa/α leu2Δ0/ leu2<sup>-</sup> lys2Δ202/LYS2 met15Δ0/MET15 ura3Δ0/ ura3<sup>-</sup> TAF14/ taf14Δ::KanMX SGO1/ sgo1Δ::HphMX &lt;pIP153&gt;</i>
JMx25		<i>MATa/α leu2Δ0/ leu2<sup>-</sup> lys2Δ202/LYS2 met15Δ0/MET15 ura3Δ0/ ura3<sup>-</sup> ARP5/ arp5Δ::KanMX SGO1/ sgo1Δ::HphMX &lt;YEplac181&gt;</i>
JMx26		<i>MATa/α leu2Δ0/ leu2<sup>-</sup> lys2Δ202/LYS2 met15Δ0/MET15 ura3Δ0/ ura3<sup>-</sup> ARP5/ arp5Δ::KanMX SGO1/ sgo1Δ::HphMX &lt;pIP153&gt;</i>
JMx27		<i>MATa/α leu2Δ0/ leu2<sup>-</sup> lys2Δ202/LYS2 met15Δ0/MET15 ura3Δ0/ ura3<sup>-</sup> INO80/ ino80Δ::KanMX SGO1/ sgo1Δ::HphMX &lt;YEplac181&gt;</i>

**Table 1. (Cont.)**

Strain or identification	Lab name	Description
JMx28		<i>MATa/α leu2Δ0/ leu2<sup>-</sup> lys2Δ202/LYS2 met15Δ0/MET15 ura3Δ0/ ura3<sup>-</sup> INO80/ ino80Δ::KanMX SGO1/ sgo1Δ::HphMX &lt;pIP153&gt;</i>
JMx13-7B <i>ies4Δ sgo1Δ</i>	IPY1211	<i>leu2<sup>-</sup> lys2Δ202 ura3<sup>-</sup> ies4Δ::KanMX sgo1Δ::HphMX</i>
JMx13-7D <i>ies4Δ sgo1Δ</i>	IPY1212	<i>leu2<sup>-</sup> met15Δ0 ura3<sup>-</sup> ies4Δ::KanMX sgo1Δ::HphMX</i>
JMx13-19A <i>ies4Δ sgo1Δ</i>	IPY1213	<i>leu2<sup>-</sup> ura3<sup>-</sup> ies4Δ::KanMX sgo1Δ::HphMX</i>
JMx13-11A <i>ies4Δ</i>	IPY1227	<i>leu2<sup>-</sup> met15Δ0 ura3<sup>-</sup> ies4Δ::KanMX</i>
JMx14-8C <i>arp8Δ sgo1Δ</i>	IPY1215	<i>leu2<sup>-</sup> met15Δ0 ura3<sup>-</sup> arp8Δ::KanMX sgo1Δ::HphMX</i>
JMx14-8D <i>arp8Δ sgo1Δ</i>	IPY1216	<i>leu2<sup>-</sup> ura3<sup>-</sup> arp8Δ::KanMX sgo1Δ::HphMX</i>
JMx14-11D <i>arp8Δ sgo1Δ</i>	IPY1214	<i>leu2<sup>-</sup> lys2Δ202 ura3<sup>-</sup> arp8Δ::KanMX sgo1Δ::HphMX</i>
JMx14-12C <i>arp8Δ</i>	IPY1228	<i>leu2<sup>-</sup> ura3<sup>-</sup> arp8Δ::KanMX</i>
JMx15-6B <i>taf14Δ sgo1Δ</i>	IPY1217	<i>leu2<sup>-</sup> lys2Δ202 met15Δ0 ura3<sup>-</sup> taf14Δ::KanMX sgo1Δ::HphMX</i>
JMx15-20B <i>taf14Δ sgo1Δ</i>	IPY1218	<i>leu2<sup>-</sup> ura3<sup>-</sup> taf14Δ::KanMX sgo1Δ::HphMX</i>
JMx15-20D <i>taf14Δ sgo1Δ</i>	IPY1219	<i>leu2<sup>-</sup> met15Δ0 ura3<sup>-</sup> taf14Δ::KanMX sgo1Δ::HphMX</i>
JMx15-2B <i>taf14Δ</i>	IPY1226	<i>leu2<sup>-</sup> lys2Δ202 met15Δ0 ura3<sup>-</sup> taf14Δ::KanMX</i>
JMx17-12B <i>ino80Δ</i>	IPY1223	<i>leu2<sup>-</sup> lys2Δ202 ura3<sup>-</sup> ino80Δ::KanMX</i>



**Table 1. (Cont.)**

Strain or identification	Lab name	Description
JMx17-19B <i>ino80Δ</i>	IPY1224	<i>leu2<sup>-</sup> met15Δ0 ura3<sup>-</sup> ino80Δ::KanMX</i>
JMx18-5D <i>ies3Δ sgo1Δ</i>		<i>leu2<sup>-</sup> met15Δ0 ura3<sup>-</sup> ies3Δ::KanMX sgo1Δ::HphMX</i>
JMx18-10A <i>ies3Δ sgo1Δ</i>		<i>leu2<sup>-</sup> lys2Δ202 ura3<sup>-</sup> ies3Δ::KanMX sgo1Δ::HphMX</i>
JMx18-12D <i>ies3Δ sgo1Δ</i>		<i>leu2<sup>-</sup> ura3<sup>-</sup> ies3Δ::KanMX sgo1Δ::HphMX</i>
JMx18-18B <i>ies3Δ</i>		<i>leu2<sup>-</sup> lys2Δ202 ura3<sup>-</sup> ies3Δ::KanMX</i>
JMx19-10B WT + YEplac181		<i>leu2<sup>-</sup> ura3<sup>-</sup> &lt;YEplac181&gt;</i>
JMx20-9B WT + pIP153		<i>leu2<sup>-</sup> ura3<sup>-</sup> &lt;pIP153&gt;</i>
JMx23-4C <i>taf14Δ</i> + YEplac181		<i>leu2<sup>-</sup> ura3<sup>-</sup> taf14Δ::KanMX &lt;YEplac181&gt;</i>
JMx23-6C <i>taf14Δ</i> + YEplac181		<i>leu2<sup>-</sup> met15Δ0 ura3<sup>-</sup> taf14Δ::KanMX &lt;YEplac181&gt;</i>
JMx24-6B <i>taf14Δ</i> + pIP153		<i>leu2<sup>-</sup> ura3<sup>-</sup> taf14Δ::KanMX &lt;pIP153&gt;</i>
JMx24-15D <i>taf14Δ</i> + pIP153		<i>leu2<sup>-</sup> lys2Δ202 met15Δ0 ura3<sup>-</sup> taf14Δ::KanMX &lt;pIP153&gt;</i>

**Table 1. (Cont.)**

Strain or identification	Lab name	Description
JMx25-9D <i>arp5Δ</i> + YEplac181		<i>leu2<sup>-</sup> lys2Δ202 ura3<sup>-</sup> arp5Δ::KanMX &lt;YEplac181&gt;</i>
JMx25-16A <i>arp5Δ</i> + YEplac181		<i>leu2<sup>-</sup> lys2Δ202 ura3<sup>-</sup> arp5Δ::KanMX &lt;YEplac181&gt;</i>
JMx26-5C <i>arp5Δ</i> + pIP153		<i>leu2<sup>-</sup> lys2Δ202 ura3<sup>-</sup> arp5Δ::KanMX &lt;pIP153&gt;</i>
JMx26-16A <i>arp5Δ</i> + pIP153		<i>leu2<sup>-</sup> lys2Δ202 ura3<sup>-</sup> arp5Δ::KanMX &lt;pIP153&gt;</i>
JMx27-4D <i>ino80Δ</i> + YEplac181		<i>leu2<sup>-</sup> lys2Δ202 met15Δ0 ura3<sup>-</sup> ino80Δ::KanMX &lt;YEplac181&gt;</i>
JMx27-8D <i>ino80Δ</i> + YEplac181		<i>leu2<sup>-</sup> lys2Δ202 ura3<sup>-</sup> ino80Δ::KanMX &lt;YEplac181&gt;</i>
JMx28-4D <i>ino80Δ</i> + pIP153		<i>leu2<sup>-</sup> met15Δ0 ura3<sup>-</sup> ino80Δ::KanMX &lt;pIP153&gt;</i>
JMx28-8D <i>ino80Δ</i> + pIP153		<i>leu2<sup>-</sup> ura3<sup>-</sup> ino80Δ::KanMX &lt;pIP153&gt;</i>

**Table 2.** Primers used in the study

Name	Sequence (5' - 3')	Purpose
oIP210	CCGTATCATGGACGATTCCTT	Forward of CEN3 core region
oIP211	TTGTCAAGTTGCTCACTGTGATT	Reverse of CEN3 core region
oIP434	ATTACGCTCGTCATCAAATCA	Reverse for Kan <sup>R</sup> deletion confirmation
oIP435	CGAAGGACTCTGAACATAAGACG	Forward of <i>ARP5</i> for deletion
oIP436	GCCGATTTGTAAACAGCACTAAG	Reverse of <i>ARP5</i> for deletion
oIP437	GACTATGATACATCATTACAACGC	Forward for confirmation of <i>arp5Δ</i>
oIP438	GAACGCCACGAAGTAGCAA	Forward of <i>ARP8</i> for deletion
oIP439	ACGCCTTCAAGTTGTGCTCC	Reverse of <i>ARP8</i> for deletion
oIP440	GCAAGATGACTTATTTGAGAATGG	Forward for confirmation of <i>arp8Δ</i>
oIP441	GTCAAGGCTGTAGTGCGGTGA	Forward of <i>TAF14</i> for deletion
oIP442	GTAAGGTGTCGCGGTTATTGGA	Reverse of <i>TAF14</i> for deletion
oIP443	CACTCAAGACGAGAAAGCTCTT	Forward for confirmation of <i>taf14Δ</i>
oIP444	GGCCGGCACTAACCACGAAT	Forward of <i>IES3</i> for deletion
oIP445	GGTAGTGCGAGAGATGGTCA	Reverse of <i>IES3</i> for deletion

**Table 2. (Cont.)**

Name	Sequence (5' - 3')	Purpose
oIP446	GGAAAACCTTGACGTCTCATCGC	Forward for confirmation of <i>ies3Δ</i>
oIP447	CGTTACGCCGTCTAGAGCTTT	Forward of <i>IES4</i> for deletion
oIP448	GGTCGGCTACCAGATTTAGTAC	Reverse of <i>IES4</i> for deletion
oIP449	GGCAGGTTACGTTGAGTAAGA	Forward for confirmation of <i>ies4Δ</i>
oIP450	GAGTAACTACCGATCCTGTCC	Forward for confirmation of <i>ino80Δ</i>
oIP451	GCGTATTCTGAGCCATCTCTC	Reverse for confirmation of <i>ino80Δ</i>
oIP452	TAGCAAAGCAAGGCTTAAGACATATAGAAGAGCATTT ATAGACGGATCCCCGGGTTAATTAA	Forward for deletion of <i>ino80Δ</i>
oIP453	ATGAAGATAGCAGATTAAGATAGACATTA ACTCCGC TTAATGAATTCGAGCTCGTTTAAAC	Reverse for deletion of <i>ino80Δ</i>
oIP454	ATAAGTCAAGATGGAATTAAGGAAGCGGCAAGTGCAT TGGCACGGATCCCCGGGTTAATTAA	Forward for C-Terminal tagging of <i>INO80</i> with 13-Myc
oIP455	TTAACTCCGCTTAATGTAAATAACACAATATGAATACC TTTTGAATTCGAGCTCGTTTAAAC	Reverse for C-Terminal tagging of <i>INO80</i> with 13-Myc
oIP464	TTGGATGAGAAGCAGCCAGGAT	Forward for confirmation of <i>nhp10Δ</i>
oIP465	TGGATAAAGCGCCTAGAACGTC	Forward for confirmation of <i>nhp10Δ</i>
oIP466	CGAATGCGGTAACGGTACAAGT	Forward for confirmation of <i>ies1Δ</i>

**Table 2. (Cont.)**

Name	Sequence (5' - 3')	Purpose
oIP467	CGTGTCCACGGTGAAGAAGAC	Forward for confirmation of <i>ies1Δ</i>
oIP468	CGCCTAACTAGCAAATAACTGGC	Forward for confirmation of <i>ies2Δ</i>
oIP469	AGTCTGCCTTACGTGGTTCTGC	Forward for confirmation of <i>ies2Δ</i>
oIP470	TGCGTTGTAACTGACATAGCTGTCTTCAATGGAATCATA ACCGGATCCCCGGGTAAATTA	Forward for deletion of <i>ies3Δ</i>
oIP471	GAAGTTGGGGATTTTGCAAACCTGTCTTATGTAAATCTTG GCGAATTCGAGCTCGTTTAAAC	Reverse for deletion of <i>ies3Δ</i>
oIP472	GGTAGTGCGAGAGATGGTCA	Forward for confirmation of <i>ies3Δ</i>
oIP473	AACCTGAGTTGAATGGCTGTGG	Forward for deletion of <i>ies5Δ</i>
oIP474	CACGCAGTGAAGGAGATTACAGA	Reverse for deletion of <i>ies5Δ</i>

**Table 3.** Plasmids used in the study

Name	Relevant genotype	Cloning vector/restriction sites
GHB160	<i>13-Myc, kanMX6</i>	pFA6a-13Myc-kanMX6
pAG25	<i>natMX6</i>	pAG25
YEplac181	<i>LEU2, 2 μ</i>	YEplac181
pIP153	<i>SGO1, LEU2, 2 μ</i>	YEplac181/ Pst1, SalI
pIP279	<i>13-Myc, natMX6</i>	pFA6a-13Myc-kanMX6/ BglII, EcoRV

**Table 4.** Phenotypical analysis of deletion mutants of INO80 and SWR1 complex.

Complex	Mutant	Canavanine test	Flow cytometry	Benomyl sensitivity
INO80	<i>ies1Δ</i>	Haploid	Haploid	-
	<i>ies2Δ</i>	Haploid	Haploid	-
	<i>ies3Δ</i>	Haploid	Haploid	-
	<i>ies4Δ</i>	Haploid	Haploid	-
	<i>ies5Δ</i>	Haploid	Haploid	-
	<i>ies6Δ</i>	Diploid	Diploid	+
	<i>nhp10Δ</i>	Haploid	Haploid	-
	<i>taf14Δ</i>	Diploid	Diploid	+
	<i>arp5Δ</i>	Diploid	Diploid	+
	<i>arp8Δ</i>	Diploid	Diploid	+
SWR1	<i>swr1Δ</i>	Diploid	Diploid	+
	<i>swc2Δ</i>	Haploid	Haploid	+
	<i>swc3Δ</i>	Haploid	Haploid	+
	<i>swc5Δ</i>	Diploid	Diploid	+
	<i>swc6Δ</i>	Diploid	Diploid	+
	<i>arp6Δ</i>	Haploid	Haploid	-
	<i>bdf1Δ</i>	Diploid	Diploid	+
Shared between SWR1 and NuA4	<i>yaf9Δ</i>	Diploid	Diploid	+
NuA4	<i>eaf1Δ</i>	Haploid	Haploid	Not tested (NT)
	<i>eaf3Δ</i>	Haploid	Haploid	NT
	<i>eaf6Δ</i>	Haploid	Haploid	NT
	<i>eaf7Δ</i>	Haploid	Haploid	NT

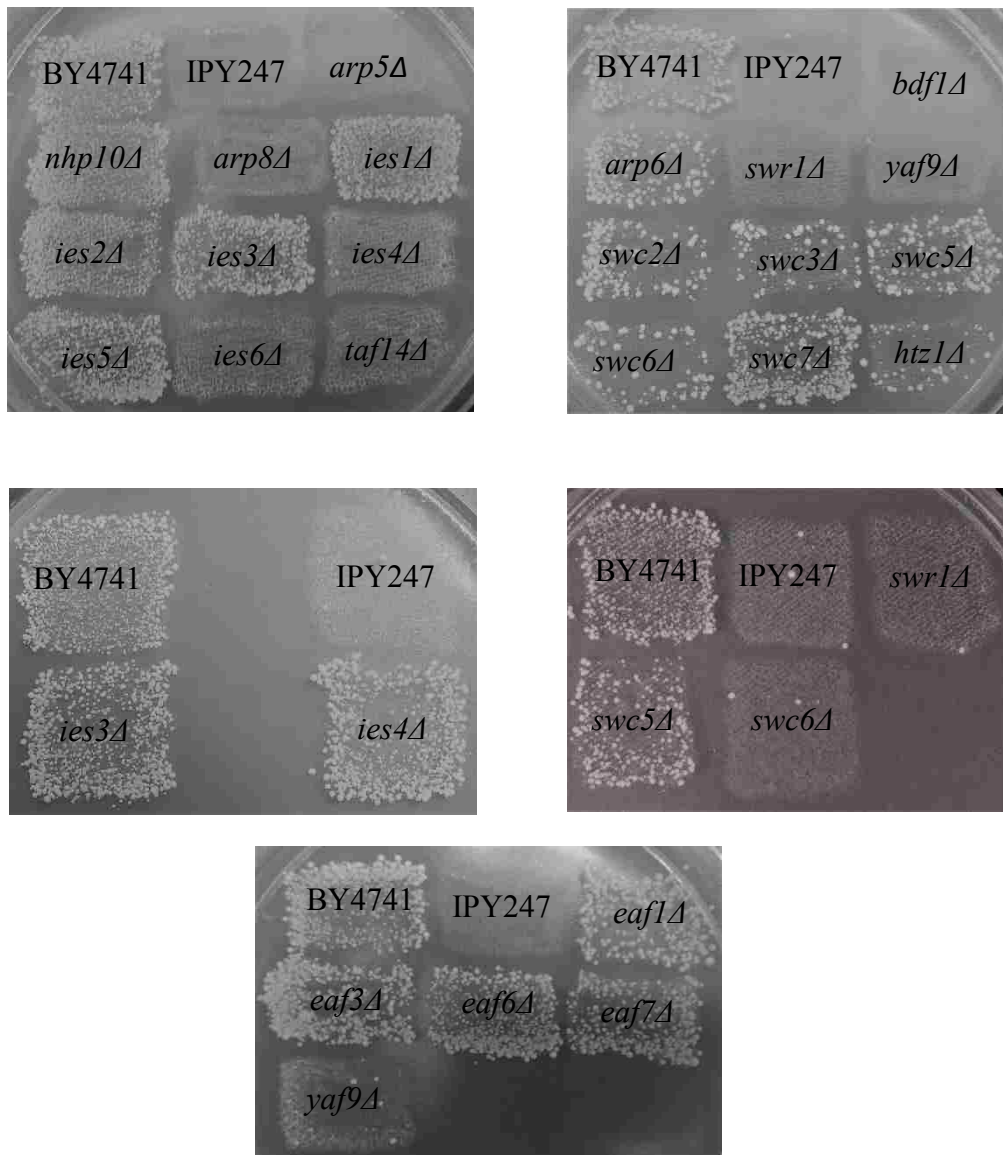


**Figure 1.** Canavanine assay for ploidy on the deletion mutants of subunits in INO80, SWR1 and NuA4 complex. Specific subunits of the complexes increase ploidy.

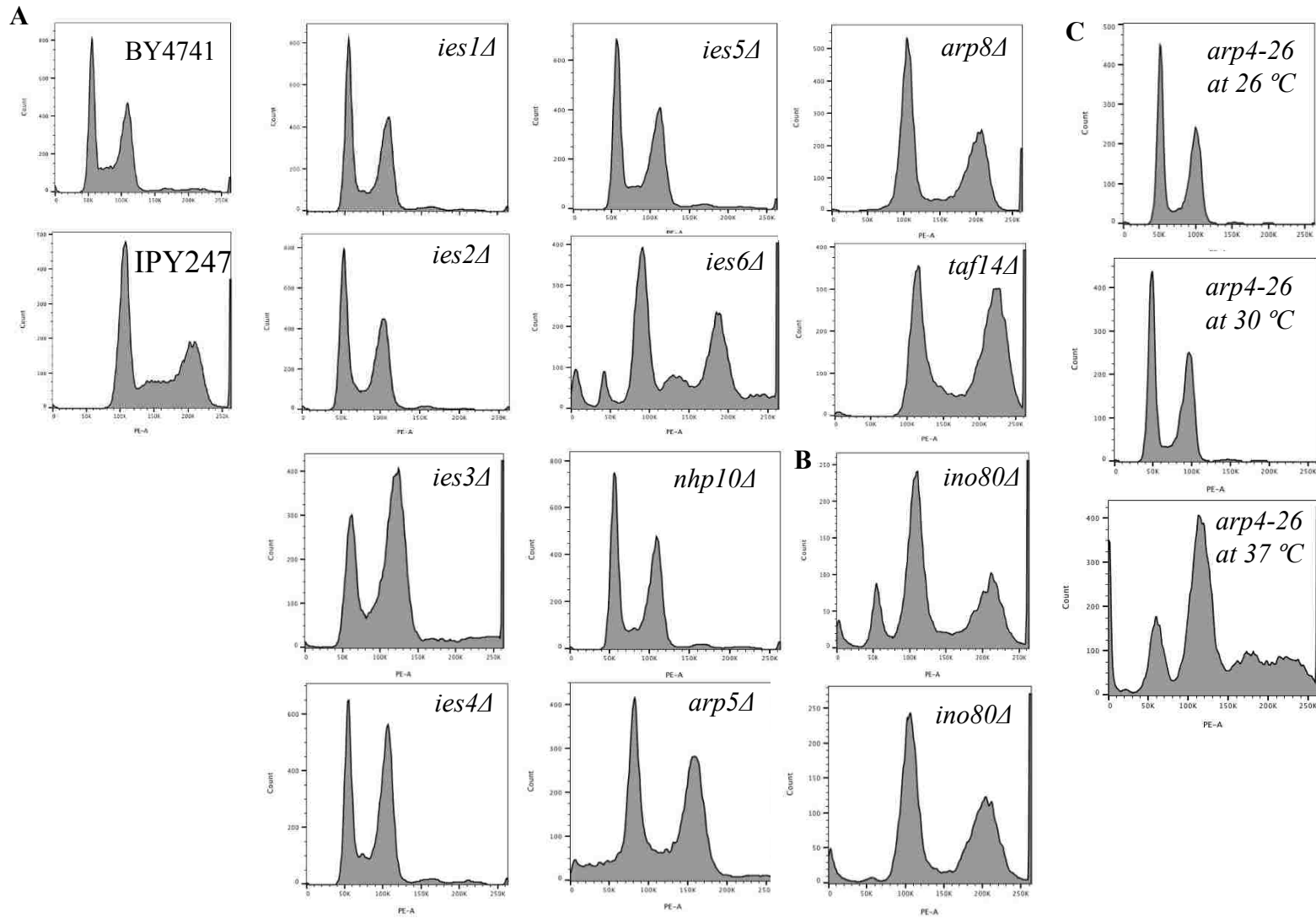


**Figure 2.** Ploidy analysis by flow cytometry in subunits of INO80 complex. A. Deletion mutants from the BY4741 background. B. Recently germinated *ino80Δ* mutants. C. Ploidy analysis of *arp4-26* mutant grew at 26, 30 and 37 °C. Increase-in-ploidy phenotype attributes to specific members of the INO80 complex.



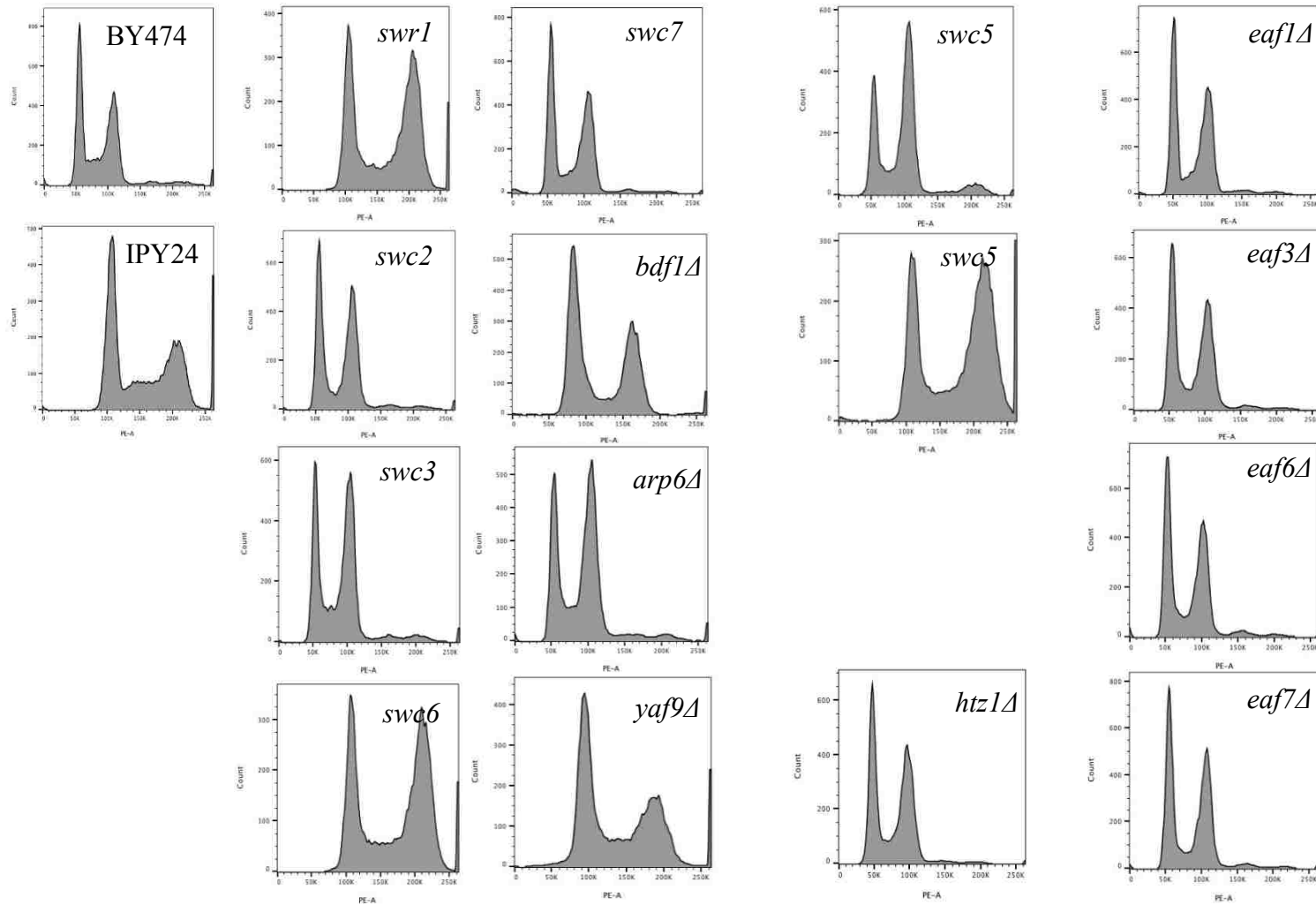


**Figure 3.** Ploidy analysis by flow cytometry in subunits of SWR1 and NuA4 complex and *HTZ1*. A. Deletion mutants of SWR1's subunits from the BY4741 background. B. Different ploidy statuses of Swc5 mutants from BY4741 background. C. Ploidy of *htz1Δ* mutant. D. Deletion mutants of NuA4's subunits from the BY4741 background

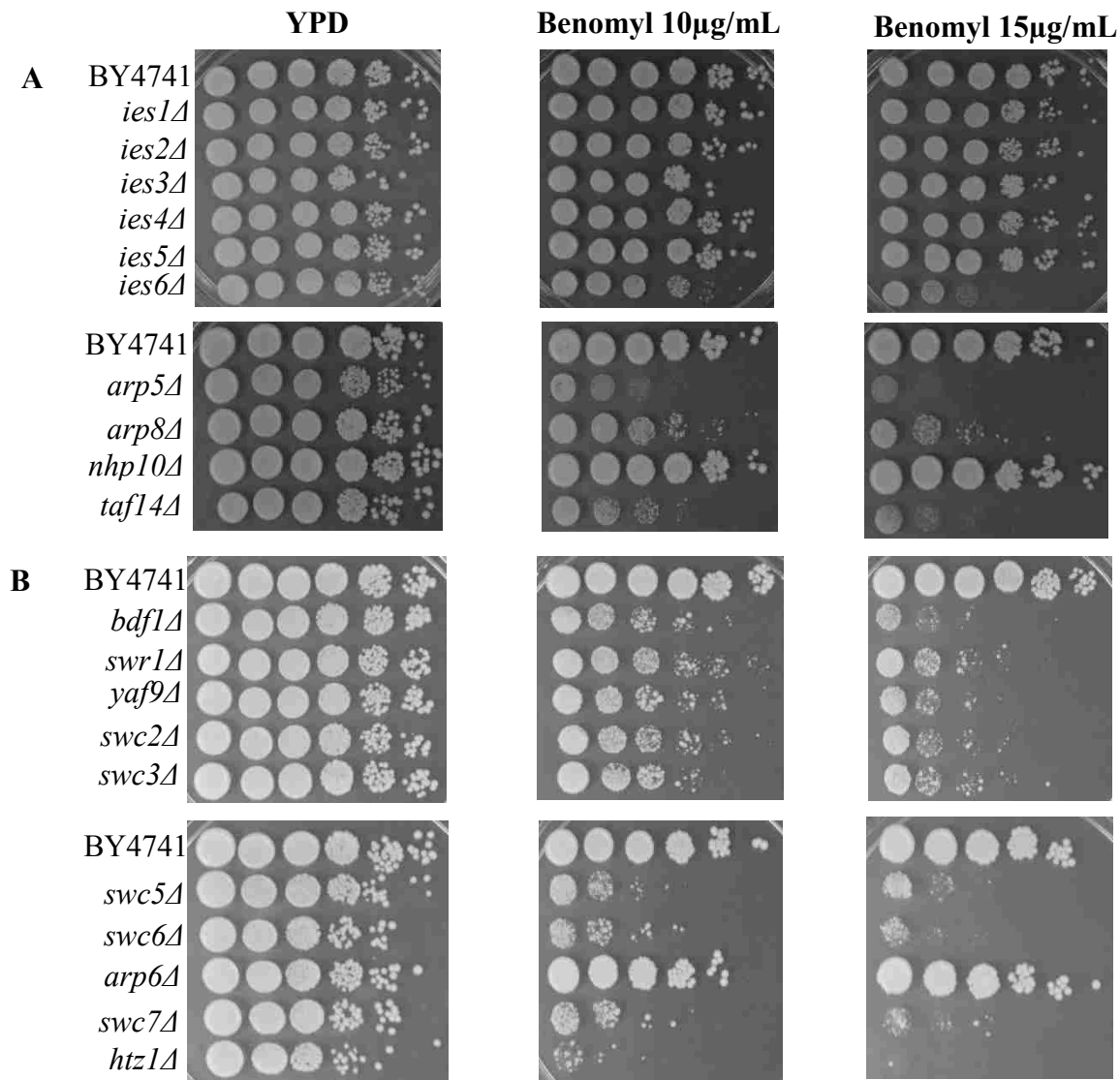


**Figure 4.** Benomyl sensitivity assay after 3 days of growth. A. Sensitivity of deleted subunits of INO80 complex from the BY4741 background. B. Sensitivity of deleted *HTZ1* and subunits of SWR1 complex from the BY4741 background.

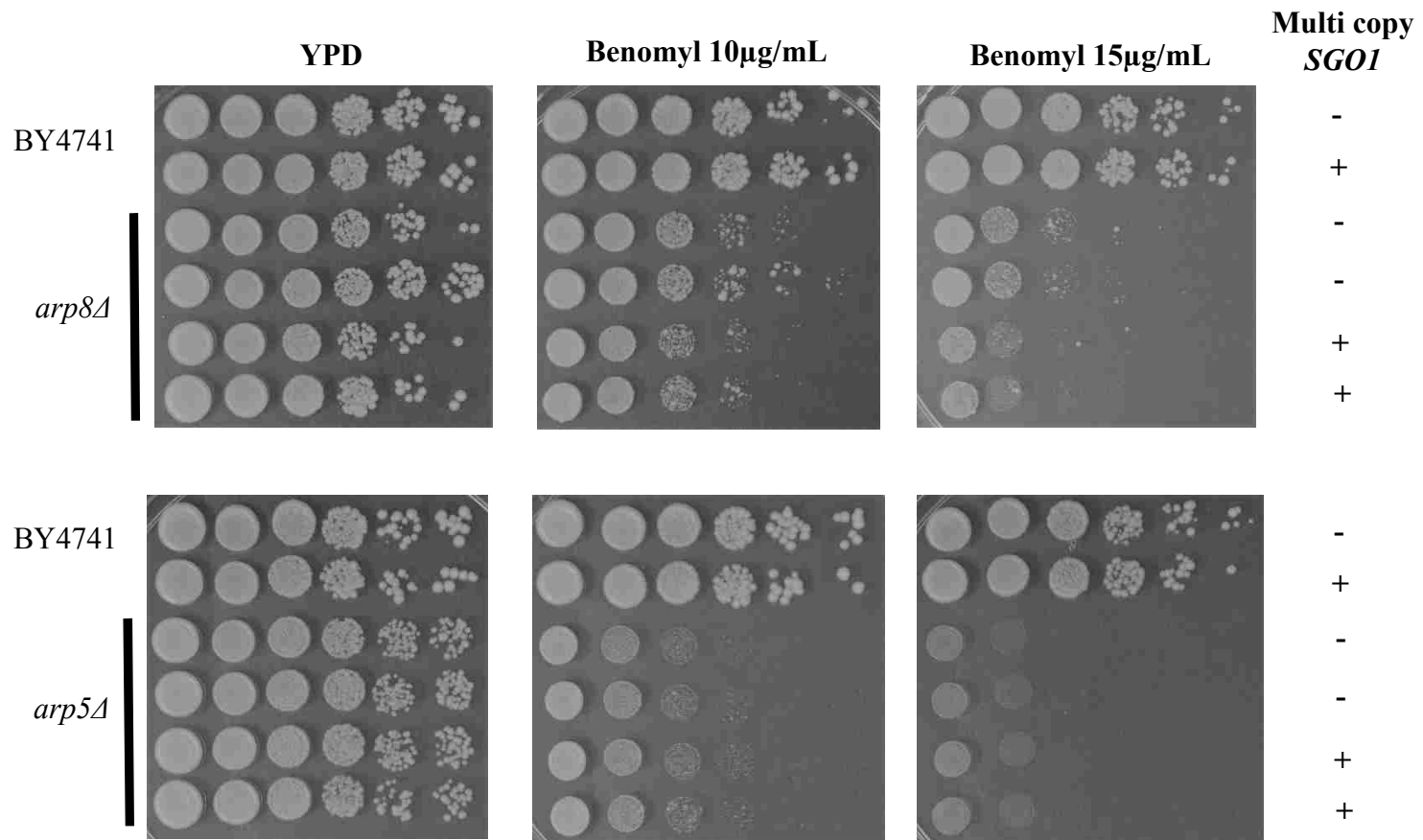


**Figure 5.** Benomyl sensitivity of *arp8* $\Delta$  and *arp5* $\Delta$  mutants containing *SGO1* in high copy.

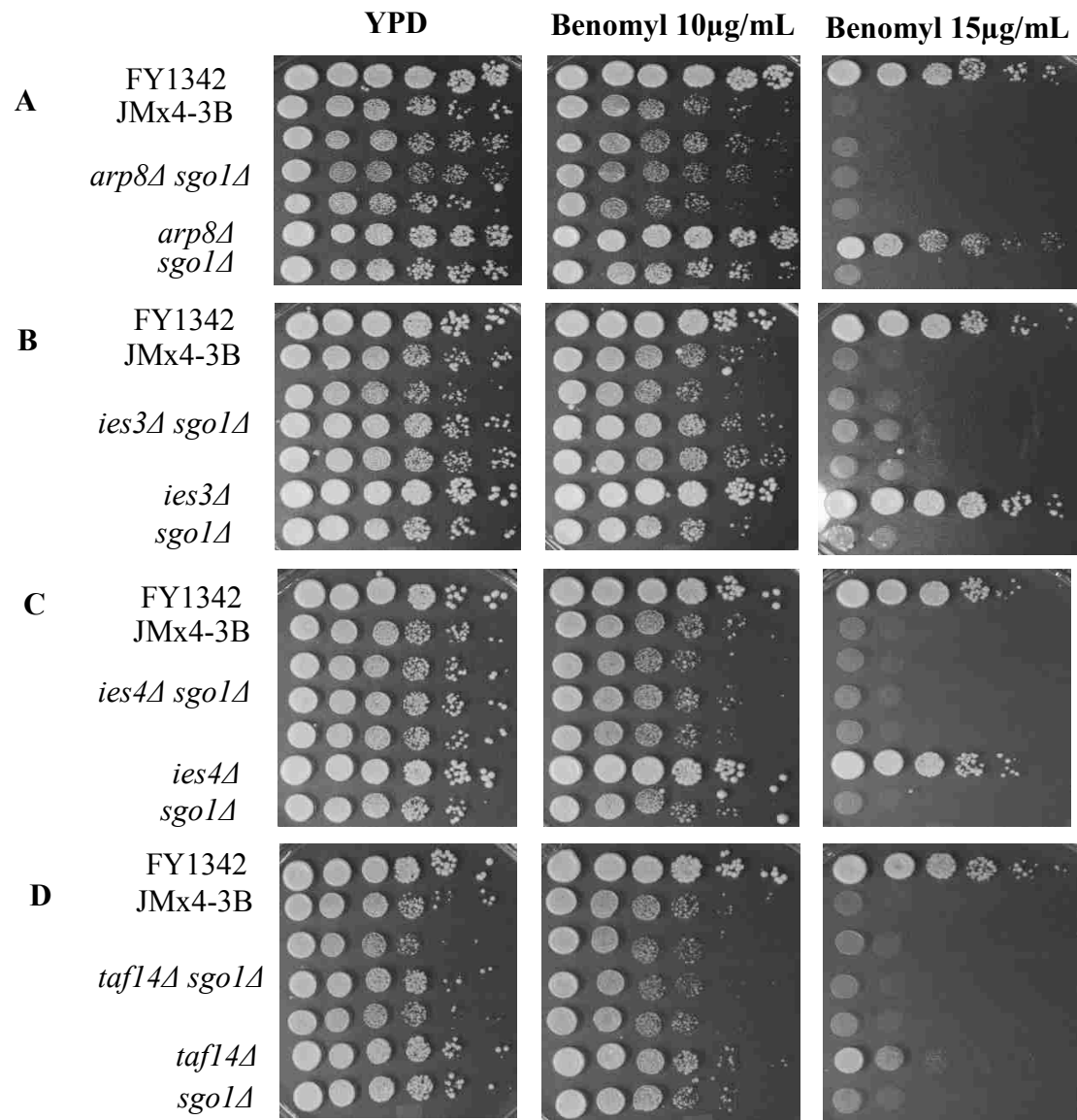


**Figure 6.** Benomyl sensitivity of double mutants. A. *arp8Δ sgo1Δ* B. *ies3Δ sgo1Δ* C. *ies4Δ sgo1Δ*. D. *taf14Δ sgo1Δ*

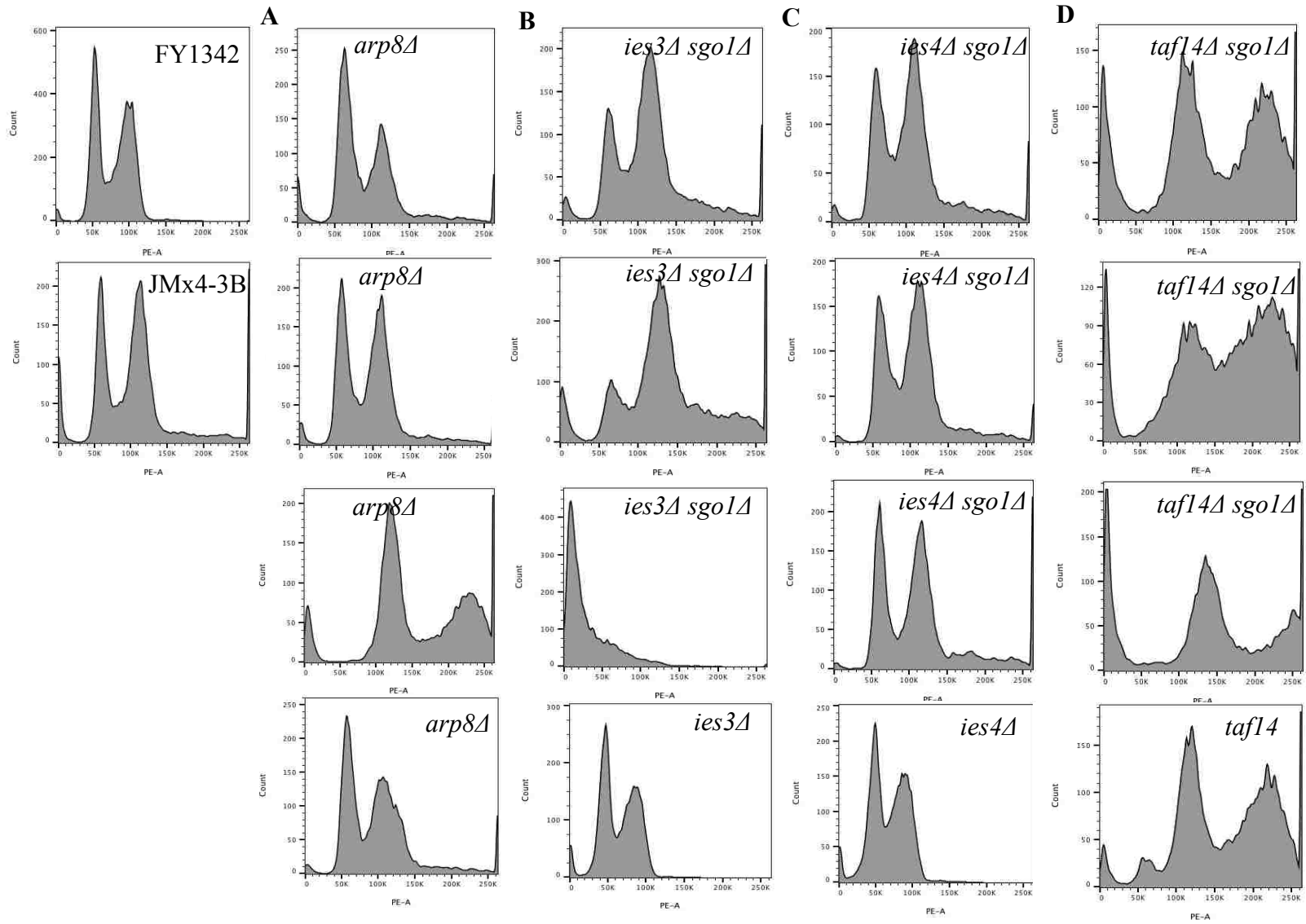


**Figure 7.** DNA content of double mutants recently germinated. A. *arp8Δ sgo1Δ* B. *ies3Δ sgo1Δ*. C. *ies4Δ sgo1Δ*. D. *taf14Δ sgo1Δ*

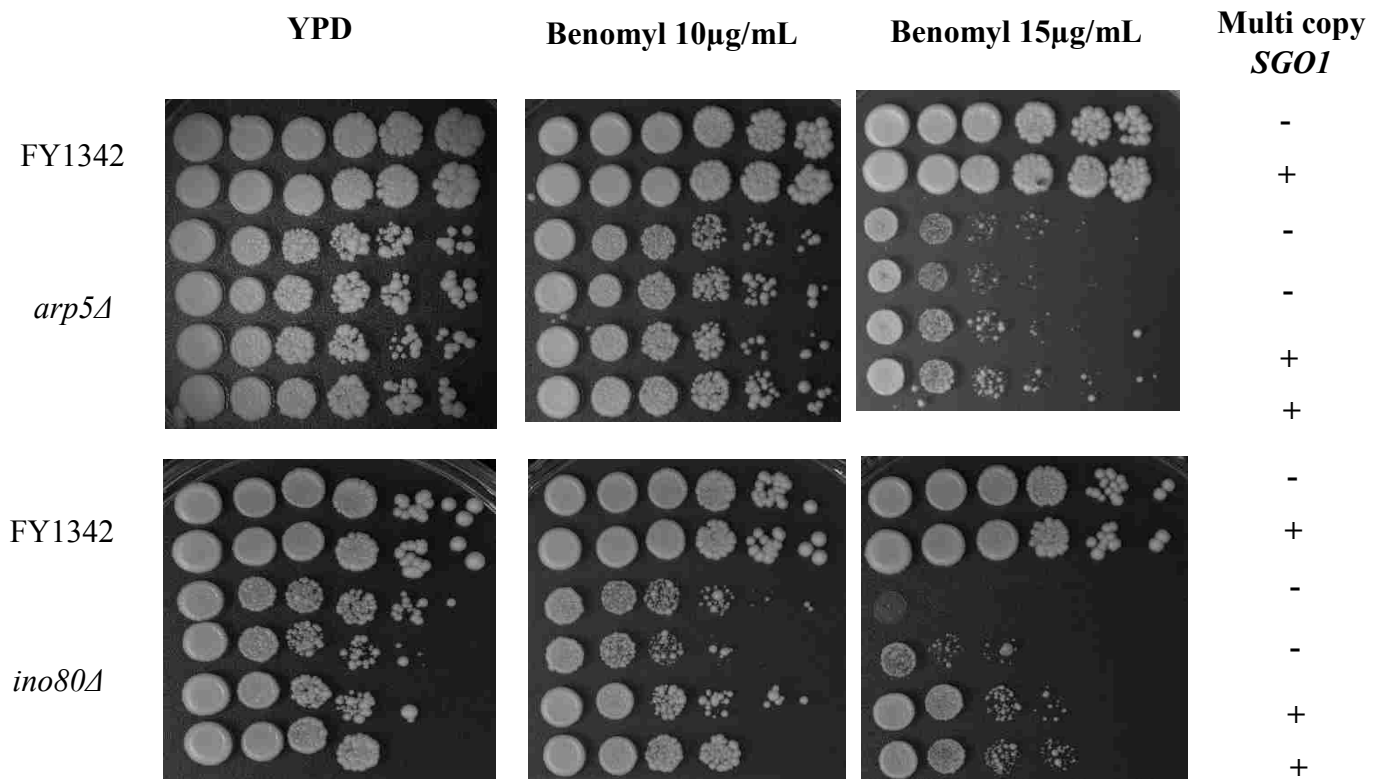


**Figure 8.** Benomyl sensitivity of *arp5* $\Delta$  and *ino80* $\Delta$  mutants that retained the high copy *SGO1* after germination.

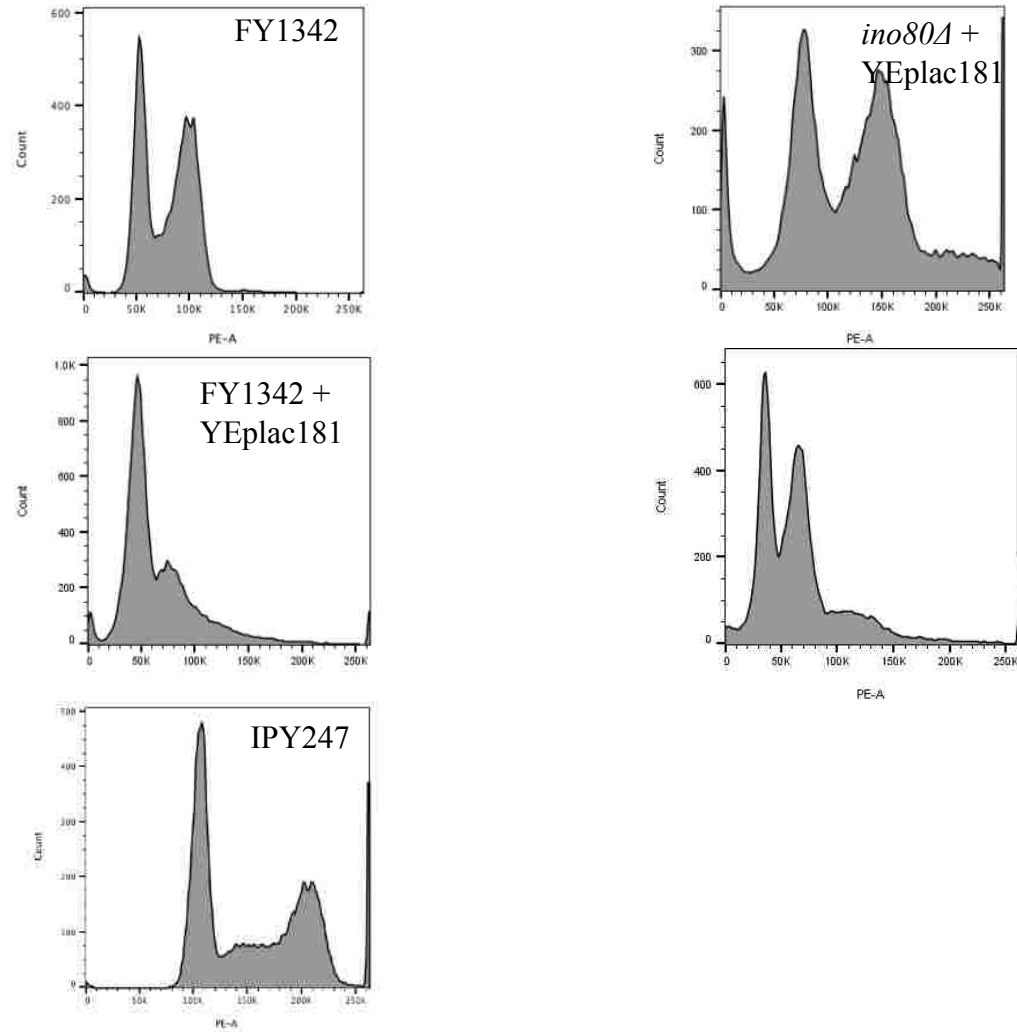


**Figure 9.** DNA content of *ino80Δ* containing *SGO1* high copy plasmid after germination. Flow cytometry analysis was performed to mid-log cells grew in selective medium for the plasmids.

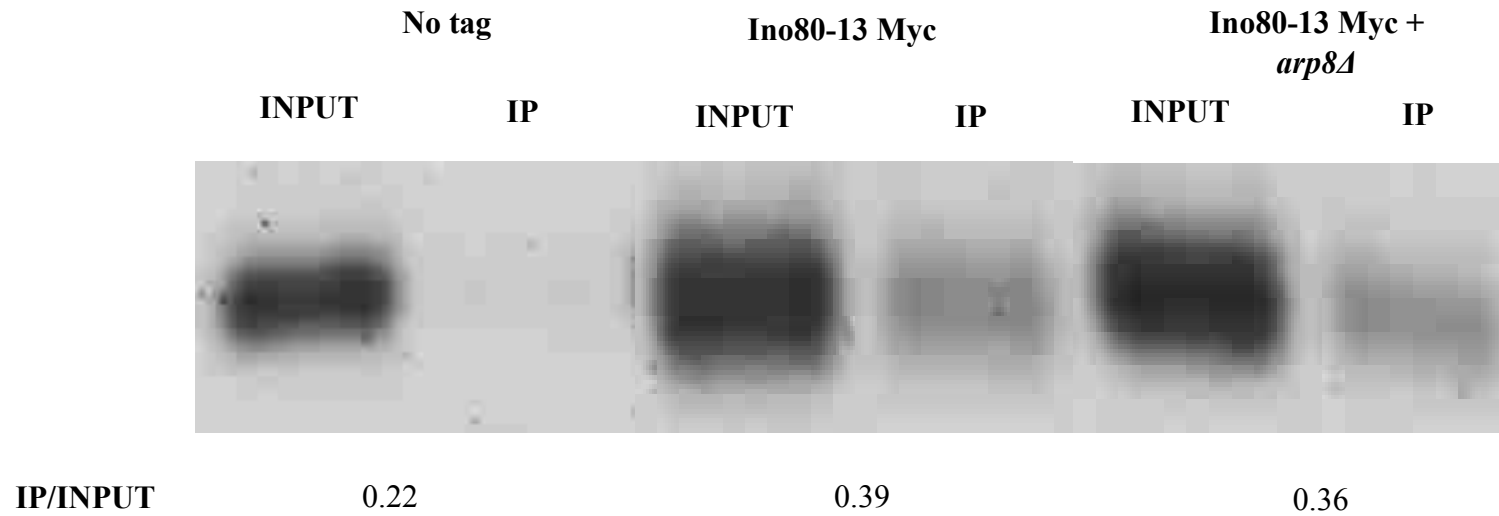


**Figure 10.** Chromatin Immunoprecipitation (ChIP) of Ino80 at the pericentromeric region of chromosome III. ChIP on Ino80-Myc was carried out with anti-myc antibodies. PCR primers used were specific for *CEN3* and a pericentromeric region (*CEN3*+ 0.5Kb left). IP/INPUT represents the relative intensity of the IP with respect of the respective input.



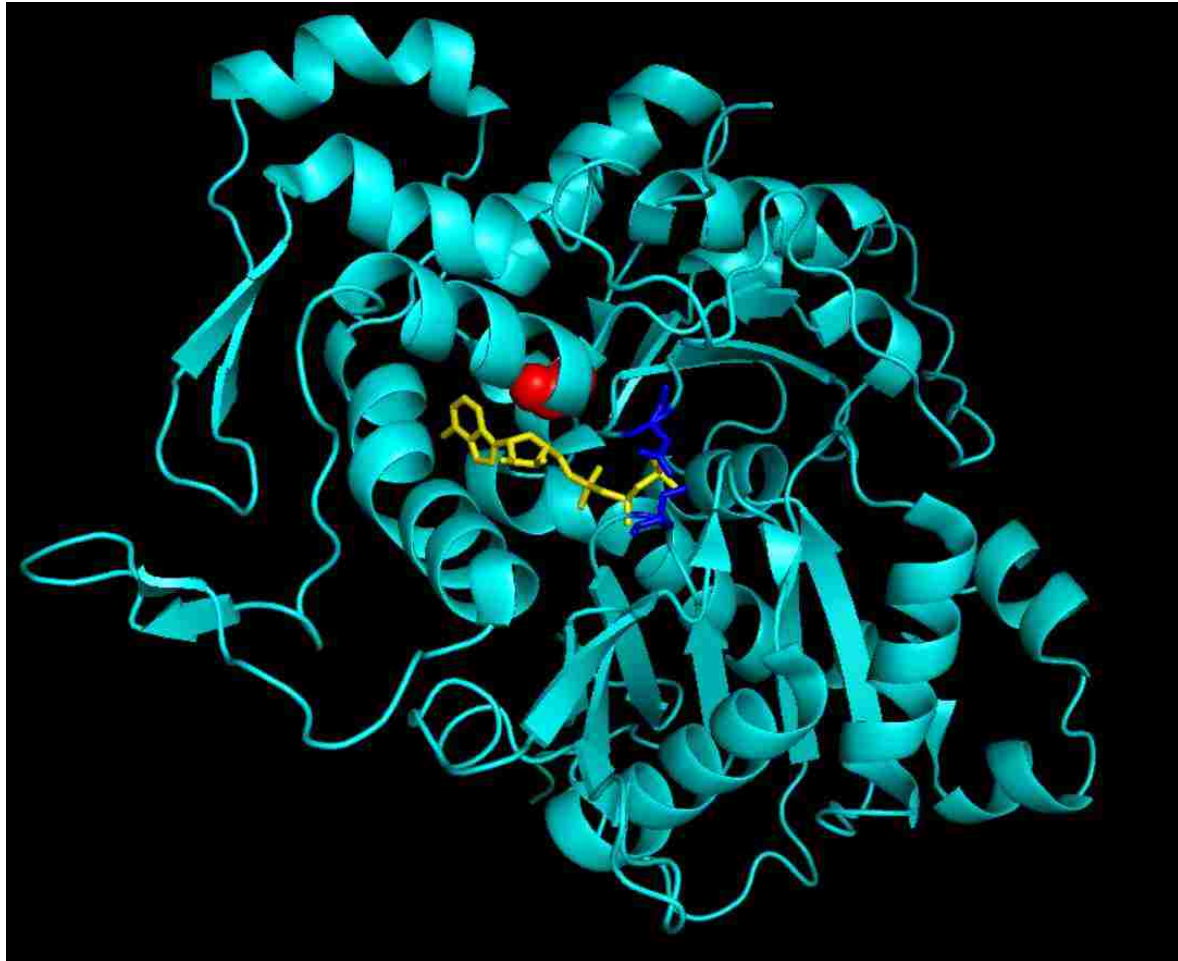


**Figure 11.** Crystal structure of Arp4. Yellow ATP bound to Arp4. Red, location of G187R mutation of arp4-26. Blue, S23 and D163 form a H-bond to tightly enclose ATP. PDB code 3QB0. Modeled using Pymol

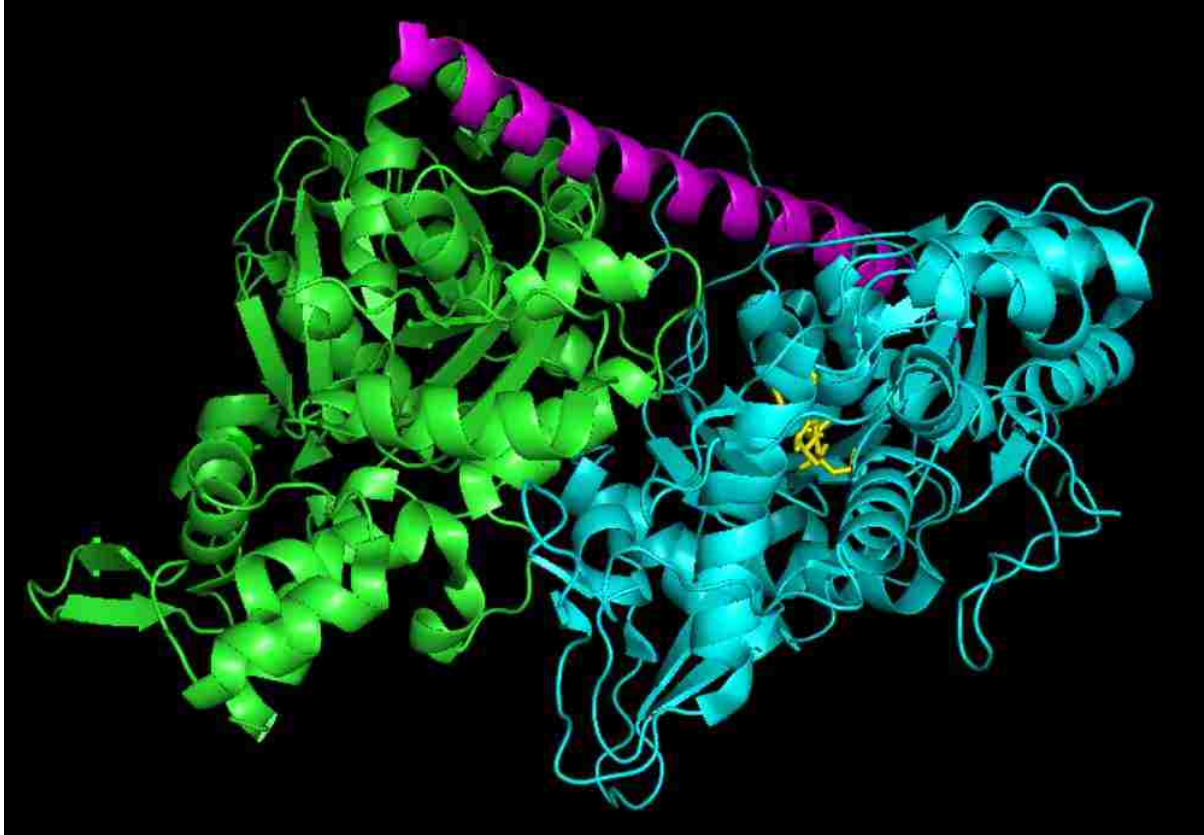


Figure 12. Ternary complex between Act1-Arp4-HSA domain. Green: Act1. Cyan: Arp4. Purple HSA domain. PDB code 5E9E. Modeled using Pymol.

## **VI. REFERENCES**

- Ahn, S. H., Henderson, K. A., Keeney, S., & Allis, C. D. (2005). H2B (Ser10) phosphorylation is induced during apoptosis and meiosis in *S. cerevisiae*. *Cell Cycle*, *4*(6), 780-783. doi:10.4161/cc.4.6.1745
- Altaf, M., Auger, A., Monnet-Saksouk, J., Brodeur, J., Piquet, S., Cramet, M., . . . Cote, J. (2010). NuA4-dependent Acetylation of Nucleosomal Histones H4 and H2A Directly Stimulates Incorporation of H2A.Z by the SWR1 Complex. *Journal of Biological Chemistry*, *285*(21), 15966-15977. doi:10.1074/jbc.M110.117069
- Antonin, W., & Neumann, H. (2016). Chromosome condensation and decondensation during mitosis. *Curr Opin Cell Biol*, *40*, 15-22. doi:10.1016/j.ceb.2016.01.013
- Au, W. C., Crisp, M. J., DeLuca, S. Z., Rando, O. J., & Basrai, M. A. (2008). Altered dosage and mislocalization of histone H3 and Cse4p lead to chromosome loss in *Saccharomyces cerevisiae*. *Genetics*, *179*(1), 263-275. doi:10.1534/genetics.108.088518
- Au, W. C., Dawson, A. R., Rawson, D. W., Taylor, S. B., Baker, R. E., & Basrai, M. A. (2013). A Novel Role of the N Terminus of Budding Yeast Histone H3 Variant Cse4 in Ubiquitin-Mediated Proteolysis. *Genetics*, *194*(2), 513-+. doi:10.1534/genetics.113.149898
- Babiarz, J. E., Halley, J. E., & Rine, J. (2006). Telomeric heterochromatin boundaries require NuA4-dependent acetylation of histone variant H2A.Z in *Saccharomyces cerevisiae*. *Genes & Development*, *20*(6), 700-710. doi:10.1101/gad.1386306
- Banerjee, T., & Chakravarti, D. (2011). A Peek into the Complex Realm of Histone Phosphorylation. *Molecular and Cellular Biology*, *31*(24), 4858-4873. doi:10.1128/mcb.05631-11
- Batta, K., Zhang, Z., Yen, K., Goffman, D. B., & Pugh, B. F. (2011). Genome-wide function of H2B ubiquitylation in promoter and genic regions. *Genes Dev*, *25*(21), 2254-2265. doi:10.1101/gad.177238.111
- Beckwith, S. L., Schwartz, E. K., García-Nieto, P. E., King, D. A., Gowans, G. J., Wong, K. M., . . . Morrison, A. J. (2018). The INO80 chromatin remodeler sustains metabolic stability by promoting TOR signaling and regulating histone acetylation. *PLoS Genet*, *14*(2), e1007216. doi:10.1371/journal.pgen.1007216
- Bi, X. (2014). Heterochromatin structure: lessons from the budding yeast. *IUBMB Life*, *66*(10), 657-666. doi:10.1002/iub.1322
- Bian, Q., & Belmont, A. S. (2012). Revisiting higher-order and large-scale chromatin organization. *Curr Opin Cell Biol*, *24*(3), 359-366. doi:10.1016/j.ceb.2012.03.003
- Billon, P., & Côté, J. (2013). Precise deposition of histone H2A.Z in chromatin for genome expression and maintenance. *Biochim Biophys Acta*, *1819*(3-4), 290-302.
- Boeckmann, L., Takahashi, Y., Au, W. C., Mishra, P. K., Choy, J. S., Dawson, A. R., . . . Basrai, M. A. (2013). Phosphorylation of centromeric histone H3 variant regulates chromosome segregation in *Saccharomyces cerevisiae*. *Molecular Biology of the Cell*, *24*(12), 2034-2044. doi:10.1091/mbc.E12-12-0893

- Botstein, D., & Fink, G. R. (2011). Yeast: an experimental organism for 21st Century biology. *Genetics*, *189*(3), 695-704. doi:10.1534/genetics.111.130765
- Bühler, M., & Gasser, S. M. (2009). Silent chromatin at the middle and ends: lessons from yeasts. *EMBO J*, *28*(15), 2149-2161. doi:10.1038/emboj.2009.185
- Cao, J., & Yan, Q. (2012). Histone ubiquitination and deubiquitination in transcription, DNA damage response, and cancer. *Front Oncol*, *2*, 26. doi:10.3389/fonc.2012.00026
- Cao, T., Sun, L., Jiang, Y., Huang, S., Wang, J., & Chen, Z. (2016). Crystal structure of a nuclear actin ternary complex. *Proc Natl Acad Sci U S A*, *113*(32), 8985-8990. doi:10.1073/pnas.1602818113
- Chambers, A. L., Ormerod, G., Durley, S. C., Sing, T. L., Brown, G. W., Kent, N. A., & Downs, J. A. (2012). The INO80 chromatin remodeling complex prevents polyploidy and maintains normal chromatin structure at centromeres. *Genes Dev*, *26*(23), 2590-2603. doi:10.1101/gad.199976.112
- Cheung, W. L., Turner, F. B., Krishnamoorthy, T., Wolner, B., Ahn, S. H., Foley, M., . . . Allis, C. D. (2005). Phosphorylation of histone H4 serine 1 during DNA damage requires casein kinase II in *S. cerevisiae*. *Curr Biol*, *15*(7), 656-660. doi:10.1016/j.cub.2005.02.049
- Clapier, C. R., & Cairns, B. R. (2009). The Biology of Chromatin Remodeling Complexes. In *Annual Review of Biochemistry* (Vol. 78, pp. 273-304). Palo Alto: Annual Reviews.
- Clarke, L., & Carbon, J. (1983). Genomic substitutions of centromeres in *Saccharomyces cerevisiae*. *Nature*, *305*(5929), 23-28.
- Darieva, Z., Webber, A., Warwood, S., & Sharrocks, A. D. (2015). Protein kinase C coordinates histone H3 phosphorylation and acetylation. *Elife*, *4*. doi:10.7554/eLife.09886
- Dhillon, N., Oki, M., Szyjka, S. J., Aparicio, O. M., & Kamakaka, R. T. (2006). H2A.Z functions to regulate progression through the cell cycle. *Mol Cell Biol*, *26*(2), 489-501. doi:10.1128/MCB.26.2.489-501.2006
- Downs, J. A., Allard, S., Jobin-Robitaille, O., Javaheri, A., Auger, A., Bouchard, N., . . . Cote, J. (2004). Binding of chromatin-modifying activities to phosphorylated histone H2A at DNA damage sites. *Molecular Cell*, *16*(6), 979-990. doi:10.1016/j.molcel.2004.12.003
- Eshleman, H. D., & Morgan, D. O. (2014). Sgo1 recruits PP2A to chromosomes to ensure sister chromatid bi-orientation during mitosis. *J Cell Sci*, *127*(Pt 22), 4974-4983. doi:10.1242/jcs.161273
- Fenn, S., Breitsprecher, D., Gerhold, C. B., Witte, G., Faix, J., & Hopfner, K. P. (2011). Structural biochemistry of nuclear actin-related proteins 4 and 8 reveals their interaction with actin. *Embo Journal*, *30*(11), 2153-2166. doi:10.1038/emboj.2011.118
- Gerhold, C. B., & Gasser, S. M. (2014). INO80 and SWR complexes: relating structure to function in chromatin remodeling. *Trends Cell Biol*, *24*(11), 619-631. doi:10.1016/j.tcb.2014.06.004

- Gietz, R. D., & Schiestl, R. H. (2007). High-efficiency yeast transformation using the LiAc/SS carrier DNA/PEG method. *Nat Protoc*, *2*(1), 31-34. doi:10.1038/nprot.2007.13
- Gietz, R. D., Schiestl, R. H., Willems, A. R., & Woods, R. A. (1995). Studies on the transformation of intact yeast cells by the LiAc/SS-DNA/PEG procedure. *Yeast*, *11*(4), 355-360. doi:10.1002/yea.320110408
- Goffeau, A., Barrell, B. G., Bussey, H., Davis, R. W., Dujon, B., Feldmann, H., . . . Oliver, S. G. (1996). Life with 6000 genes. *Science*, *274*(5287), 546, 563-547.
- Haase, J., Stephens, A., Verdaasdonk, J., Yeh, E., & Bloom, K. (2012). Bub1 Kinase and Sgo1 Modulate Pericentric Chromatin in Response to Altered Microtubule Dynamics. *Current Biology*, *22*(6), 471-481. doi:10.1016/j.cub.2012.02.006
- Harikumar, A., & Meshorer, E. (2015). Chromatin remodeling and bivalent histone modifications in embryonic stem cells. *EMBO Rep*, *16*(12), 1609-1619. doi:10.15252/embr.201541011
- Hildebrand, E. M., & Biggins, S. (2016). Regulation of Budding Yeast CENP-A levels Prevents Misincorporation at Promoter Nucleosomes and Transcriptional Defects. *PLoS Genet*, *12*(3), e1005930. doi:10.1371/journal.pgen.1005930
- Hou, H. T., Wang, Y., Kallgren, S. P., Thompson, J., Yates, J. R., & Jia, S. T. (2010). Histone Variant H2A.Z Regulates Centromere Silencing and Chromosome Segregation in Fission Yeast. *Journal of Biological Chemistry*, *285*(3), 1909-1918. doi:10.1074/jbc.M109.058487
- Hsu, J. Y., Sun, Z. W., Li, X., Reuben, M., Tatchell, K., Bishop, D. K., . . . Allis, C. D. (2000). Mitotic phosphorylation of histone H3 is governed by Ipl1/aurora kinase and Glc7/PP1 phosphatase in budding yeast and nematodes. *Cell*, *102*(3), 279-291.
- Huang, F., Ramakrishnan, S., Pokhrel, S., Pflueger, C., Parnell, T. J., Kasten, M. M., . . . Chandrasekharan, M. B. (2015). Interaction of the Jhd2 Histone H3 Lys-4 Demethylase with Chromatin Is Controlled by Histone H2A Surfaces and Restricted by H2B Ubiquitination. *J Biol Chem*, *290*(48), 28760-28777. doi:10.1074/jbc.M115.693085
- Hur, S. K., Park, E. J., Han, J. E., Kim, Y. A., Kim, J. D., Kang, D., & Kwon, J. (2010). Roles of human INO80 chromatin remodeling enzyme in DNA replication and chromosome segregation suppress genome instability. *Cell Mol Life Sci*, *67*(13), 2283-2296. doi:10.1007/s00018-010-0337-3
- Jaiswal, D., Turniansky, R., & Green, E. M. (2017). Choose Your Own Adventure: The Role of Histone Modifications in Yeast Cell Fate. *J Mol Biol*, *429*(13), 1946-1957. doi:10.1016/j.jmb.2016.10.018
- Jeronimo, C., Watanabe, S., Kaplan, C. D., Peterson, C. L., & Robert, F. (2015). The Histone Chaperones FACT and Spt6 Restrict H2A.Z from Intragenic Locations. *Mol Cell*, *58*(6), 1113-1123. doi:10.1016/j.molcel.2015.03.030
- Kalocsay, M., Hiller, N. J., & Jentsch, S. (2009). Chromosome-wide Rad51 spreading and SUMO-H2A.Z-dependent chromosome fixation in response to a persistent DNA double-strand break. *Mol Cell*, *33*(3), 335-343. doi:10.1016/j.molcel.2009.01.016

- Kanta, H., Laprade, L., Almutairi, A., & Pinto, I. (2006). Suppressor analysis of a histone defect identifies a new function for the hda1 complex in chromosome segregation. *Genetics*, *173*(1), 435-450. doi:10.1534/genetics.105.050559
- Kawashima, S., Nakabayashi, Y., Matsubara, K., Sano, N., Enomoto, T., Tanaka, K., . . . Horikoshi, M. (2011). Global analysis of core histones reveals nucleosomal surfaces required for chromosome bi-orientation. *EMBO J*, *30*(16), 3353-3367. doi:10.1038/emboj.2011.241
- Kawashima, S. A., Yamagishi, Y., Honda, T., Ishiguro, K., & Watanabe, Y. (2010). Phosphorylation of H2A by Bub1 prevents chromosomal instability through localizing shugoshin. *Science*, *327*(5962), 172-177. doi:10.1126/science.1180189
- Krenn, V., & Musacchio, A. (2015). The Aurora B Kinase in Chromosome Bi-Orientation and Spindle Checkpoint Signaling. *Front Oncol*, *5*, 225. doi:10.3389/fonc.2015.00225
- Lademann, C. A., Renkawitz, J., Pfander, B., & Jentsch, S. (2017). The INO80 Complex Removes H2A.Z to Promote Presynaptic Filament Formation during Homologous Recombination. *Cell Rep*, *19*(7), 1294-1303. doi:10.1016/j.celrep.2017.04.051
- Li, G., & Reinberg, D. (2011). Chromatin higher-order structures and gene regulation. *Curr Opin Genet Dev*, *21*(2), 175-186. doi:10.1016/j.gde.2011.01.022
- Li, Q., Zhou, H., Wurtele, H., Davies, B., Horazdovsky, B., Verreault, A., & Zhang, Z. (2008). Acetylation of histone H3 lysine 56 regulates replication-coupled nucleosome assembly. *Cell*, *134*(2), 244-255. doi:10.1016/j.cell.2008.06.018
- Luger, K., Mäder, A. W., Richmond, R. K., Sargent, D. F., & Richmond, T. J. (1997). Crystal structure of the nucleosome core particle at 2.8 Å resolution. *Nature*, *389*(6648), 251-260. doi:10.1038/38444
- Mahajan, K., Fang, B., Koomen, J. M., & Mahajan, N. P. (2012). H2B Tyr37 phosphorylation suppresses expression of replication-dependent core histone genes. *Nat Struct Mol Biol*, *19*(9), 930-937. doi:10.1038/nsmb.2356
- Martins-Taylor, K., Sharma, U., Rozario, T., & Holmes, S. G. (2011). H2A.Z (Htz1) Controls the Cell-Cycle-Dependent Establishment of Transcriptional Silencing at *Saccharomyces cerevisiae* Telomeres. *Genetics*, *187*(1), 89-104. doi:10.1534/genetics.110.123844
- McGinty, R. K., & Tan, S. (2015). Nucleosome structure and function. *Chem Rev*, *115*(6), 2255-2273. doi:10.1021/cr500373h
- Meneghini, M. D., Wu, M., & Madhani, H. D. (2003). Conserved histone variant H2A.Z protects euchromatin from the ectopic spread of silent heterochromatin. *Cell*, *112*(5), 725-736.
- Morey, L., Barnes, K., Chen, Y. H., Fitzgerald-Hayes, M., & Baker, R. E. (2004). The histone fold domain of Cse4 is sufficient for CEN targeting and propagation of active centromeres in budding yeast. *Eukaryotic Cell*, *3*(6), 1533-1543. doi:10.1128/ec.3.6.1533-1543.2004

- Morrison, A. J., Highland, J., Krogan, N. J., Arbel-Eden, A., Greenblatt, J. F., Haber, J. E., & Shen, X. (2004). INO80 and gamma-H2AX interaction links ATP-dependent chromatin remodeling to DNA damage repair. *Cell*, *119*(6), 767-775. doi:10.1016/j.cell.2004.11.037
- Morrison, A. J., & Shen, X. (2009). Chromatin remodelling beyond transcription: the INO80 and SWR1 complexes. *Nat Rev Mol Cell Biol*, *10*(6), 373-384. doi:10.1038/nrm2693
- Nakagawa, T., Kajitani, T., Togo, S., Masuko, N., Ohdan, H., Hishikawa, Y., . . . Ito, T. (2008). Deubiquitylation of histone H2A activates transcriptional initiation via trans-histone cross-talk with H3K4 di- and trimethylation. *Genes Dev*, *22*(1), 37-49. doi:10.1101/gad.1609708
- Ng, H. H., Xu, R. M., Zhang, Y., & Struhl, K. (2002). Ubiquitination of histone H2B by Rad6 is required for efficient Dot1-mediated methylation of histone H3 lysine 79. *J Biol Chem*, *277*(38), 34655-34657. doi:10.1074/jbc.C200433200
- Ogiwara, H., Enomoto, T., & Seki, M. (2007). The INO80 chromatin remodeling complex functions in sister chromatid cohesion. *Cell Cycle*, *6*(9), 1090-1095. doi:10.4161/cc.6.9.4130
- Papamichos-Chronakis, M., Watanabe, S., Rando, O. J., & Peterson, C. L. (2011). Global regulation of H2A.Z localization by the INO80 chromatin-remodeling enzyme is essential for genome integrity. *Cell*, *144*(2), 200-213. doi:10.1016/j.cell.2010.12.021
- Pearson, C. G., Yeh, E., Gardner, M., Odde, D., Salmon, E. D., & Bloom, K. (2004). Stable kinetochore-microtubule attachment constrains centromere positioning in metaphase. *Curr Biol*, *14*(21), 1962-1967. doi:10.1016/j.cub.2004.09.086
- Peplowska, K., Wallek, A. U., & Storchova, Z. (2014). Sgo1 regulates both condensin and Ipl1/Aurora B to promote chromosome biorientation. *PLoS Genet*, *10*(6), e1004411. doi:10.1371/journal.pgen.1004411
- Pokholok, D. K., Harbison, C. T., Levine, S., Cole, M., Hannett, N. M., Lee, T. I., . . . Young, R. A. (2005). Genome-wide map of nucleosome acetylation and methylation in yeast. *Cell*, *122*(4), 517-527. doi:10.1016/j.cell.2005.06.026
- Poli, J., Gasser, S. M., & Papamichos-Chronakis, M. (2017). The INO80 remodeler in transcription, replication and repair. *Philos Trans R Soc Lond B Biol Sci*, *372*(1731). doi:10.1098/rstb.2016.0290
- Prakash, K., & Fournier, D. (2018). Evidence for the implication of the histone code in building the genome structure. *Biosystems*, *164*, 49-59. doi:10.1016/j.biosystems.2017.11.005
- Robzyk, K., Recht, J., & Osley, M. A. (2000). Rad6-dependent ubiquitination of histone H2B in yeast. *Science*, *287*(5452), 501-504.
- Rose, M. D., Winston F. and Hieter P., (1990). *Methods in yeast genetics: A laboratory course manual*. Cold Spring Harbor, NY: Cold Spring Harbor Laboratory Pres.
- Rossetto, D., Avvakumov, N., & Cote, J. (2012). Histone phosphorylation A chromatin modification involved in diverse nuclear events. *Epigenetics*, *7*(10), 1098-1108. doi:10.4161/epi.21975



- Ryan, D. P., & Owen-Hughes, T. (2011). Snf2-family proteins: chromatin remodellers for any occasion. *Curr Opin Chem Biol*, *15*(5), 649-656. doi:10.1016/j.cbpa.2011.07.022
- Sambrook J., F. E. F., and Maniatis T.,. (1989). *Molecular cloning: A laboratory manual*. Cold Spring Harbor, NY: Cold Spring Harbor Press.
- Shen, X., Ranallo, R., Choi, E., & Wu, C. (2003). Involvement of actin-related proteins in ATP-dependent chromatin remodeling. *Mol Cell*, *12*(1), 147-155.
- Shen, X., Xiao, H., Ranallo, R., Wu, W. H., & Wu, C. (2003). Modulation of ATP-dependent chromatin-remodeling complexes by inositol polyphosphates. *Science*, *299*(5603), 112-114. doi:10.1126/science.1078068
- Shimada, K., Oma, Y., Schleker, T., Kugou, K., Ohta, K., Harata, M., & Gasser, S. M. (2008). Ino80 chromatin remodeling complex promotes recovery of stalled replication forks. *Curr Biol*, *18*(8), 566-575. doi:10.1016/j.cub.2008.03.049
- Shivaraju, M., Unruh, J. R., Slaughter, B. D., Mattingly, M., Berman, J., & Gerton, J. L. (2012). Cell-Cycle-Coupled Structural Oscillation of Centromeric Nucleosomes in Yeast. *Cell*, *150*(2), 304-316. doi:10.1016/j.cell.2012.05.034
- Stoler, S., Keith, K. C., Curnick, K. E., & Fitzgerald-Hayes, M. (1995). A MUTATION IN CSE4, AN ESSENTIAL GENE ENCODING A NOVEL CHROMATIN-ASSOCIATED PROTEIN IN YEAST, CAUSES CHROMOSOME NONDISJUNCTION AND CELL-CYCLE ARREST AT MITOSIS. *Genes & Development*, *9*(5), 573-586. doi:10.1101/gad.9.5.573
- Storchová, Z., Becker, J. S., Talarek, N., Kögelsberger, S., & Pellman, D. (2011). Bub1, Sgo1, and Mps1 mediate a distinct pathway for chromosome biorientation in budding yeast. *Mol Biol Cell*, *22*(9), 1473-1485. doi:10.1091/mbc.E10-08-0673
- Strahl, B. D., & Allis, C. D. (2000). The language of covalent histone modifications. *Nature*, *403*(6765), 41-45. doi:10.1038/47412
- Sun, Z. W., & Allis, C. D. (2002). Ubiquitination of histone H2B regulates H3 methylation and gene silencing in yeast. *Nature*, *418*(6893), 104-108. doi:10.1038/nature00883
- Szerlong, H., Hinata, K., Viswanathan, R., Erdjument-Bromage, H., Tempst, P., & Cairns, B. R. (2008). The HSA domain binds nuclear actin-related proteins to regulate chromatin-remodeling ATPases. *Nat Struct Mol Biol*, *15*(5), 469-476. doi:10.1038/nsmb.1403
- Tanaka, T. U., Stark, M. J., & Tanaka, K. (2005). Kinetochores capture and bi-orientation on the mitotic spindle. *Nat Rev Mol Cell Biol*, *6*(12), 929-942. doi:10.1038/nrm1764
- Thurtle, D. M., & Rine, J. (2014). The molecular topography of silenced chromatin in *Saccharomyces cerevisiae*. *Genes Dev*, *28*(3), 245-258. doi:10.1101/gad.230532.113
- Tosi, A., Haas, C., Herzog, F., Gilmozzi, A., Berninghausen, O., Ungewickell, C., . . . Hopfner, K. P. (2013). Structure and subunit topology of the INO80 chromatin remodeler and its nucleosome complex. *Cell*, *154*(6), 1207-1219. doi:10.1016/j.cell.2013.08.016

- Tramantano, M., Sun, L., Au, C., Labuz, D., Liu, Z., Chou, M., . . . Luk, E. (2016). Constitutive turnover of histone H2A.Z at yeast promoters requires the preinitiation complex. *Elife*, 5. doi:10.7554/eLife.14243
- Udugama, M., Sabri, A., & Bartholomew, B. (2011). The INO80 ATP-dependent chromatin remodeling complex is a nucleosome spacing factor. *Mol Cell Biol*, 31(4), 662-673. doi:10.1128/MCB.01035-10
- van Attikum, H., Fritsch, O., Hohn, B., & Gasser, S. M. (2004). Recruitment of the INO80 complex by H2A phosphorylation links ATP-dependent chromatin remodeling with DNA double-strand break repair. *Cell*, 119(6), 777-788. doi:10.1016/j.cell.2004.11.033
- Verdaasdonk, J. S., & Bloom, K. (2011). Centromeres: unique chromatin structures that drive chromosome segregation. *Nat Rev Mol Cell Biol*, 12(5), 320-332. doi:10.1038/nrm3107
- Wang, X., & Dai, W. (2005). Shugoshin, a guardian for sister chromatid segregation. *Exp Cell Res*, 310(1), 1-9. doi:10.1016/j.yexcr.2005.07.018
- Wilkins, B. J., Rall, N. A., Ostwal, Y., Kruitwagen, T., Hiragami-Hamada, K., Winkler, M., . . . Neumann, H. (2014). A cascade of histone modifications induces chromatin condensation in mitosis. *Science*, 343(6166), 77-80. doi:10.1126/science.1244508
- Willhoft, O., Bythell-Douglas, R., McCormack, E. A., & Wigley, D. B. (2016). Synergy and antagonism in regulation of recombinant human INO80 chromatin remodeling complex. *Nucleic Acids Res*, 44(17), 8179-8188. doi:10.1093/nar/gkw509
- Williamson, W. D., & Pinto, I. (2012). Histones and genome integrity. *Front Biosci (Landmark Ed)*, 17, 984-995.
- Winston, F., Dollard, C., & Ricupero-Hovasse, S. L. (1995). Construction of a set of convenient *Saccharomyces cerevisiae* strains that are isogenic to S288C. *Yeast*, 11(1), 53-55. doi:10.1002/yea.320110107
- Wyce, A., Xiao, T., Whelan, K. A., Kosman, C., Walter, W., Eick, D., . . . Berger, S. L. (2007). H2B ubiquitylation acts as a barrier to Ctk1 nucleosomal recruitment prior to removal by Ubp8 within a SAGA-related complex. *Mol Cell*, 27(2), 275-288. doi:10.1016/j.molcel.2007.01.035
- Xue, Y., Van, C., Pradhan, S. K., Su, T., Gehrke, J., Kuryan, B. G., . . . Carey, M. F. (2015). The Ino80 complex prevents invasion of euchromatin into silent chromatin. *Genes Dev*, 29(4), 350-355. doi:10.1101/gad.256255.114
- Yamagishi, Y., Sakuno, T., Shimura, M., & Watanabe, Y. (2008). Heterochromatin links to centromeric protection by recruiting shugoshin. *Nature*, 455(7210), 251-255. doi:10.1038/nature07217
- Yao, W., Beckwith, S. L., Zheng, T., Young, T., Dinh, V. T., Ranjan, A., & Morrison, A. J. (2015). Assembly of the Arp5 (Actin-related Protein) Subunit Involved in Distinct INO80 Chromatin Remodeling Activities. *J Biol Chem*, 290(42), 25700-25709. doi:10.1074/jbc.M115.674887

- Yao, W., King, D. A., Beckwith, S. L., Gowans, G. J., Yen, K., Zhou, C., & Morrison, A. J. (2016). The INO80 Complex Requires the Arp5-Ies6 Subcomplex for Chromatin Remodeling and Metabolic Regulation. *Mol Cell Biol*, 36(6), 979-991. doi:10.1128/MCB.00801-15
- Yao, Y., & Dai, W. (2012). Shugoshins function as a guardian for chromosomal stability in nuclear division. *Cell Cycle*, 11(14), 2631-2642. doi:10.4161/cc.20633